AD-A060 302 MASSACHUSETTS INST OF TECH CAMBRIDGE DEPT OF OCEAN E--ETC F/G 13/13
A NUMERICAL PROCEDURE FOR THE DYNAMIC PLASTIC RESPONSE OF BEAMS--ETC(U).
AUG 78 J G DE OLIVEIRA, N JONES N00014-76-C-0195

UNCLASSIFIED 78-2 NL

| OF |
ADA
060302

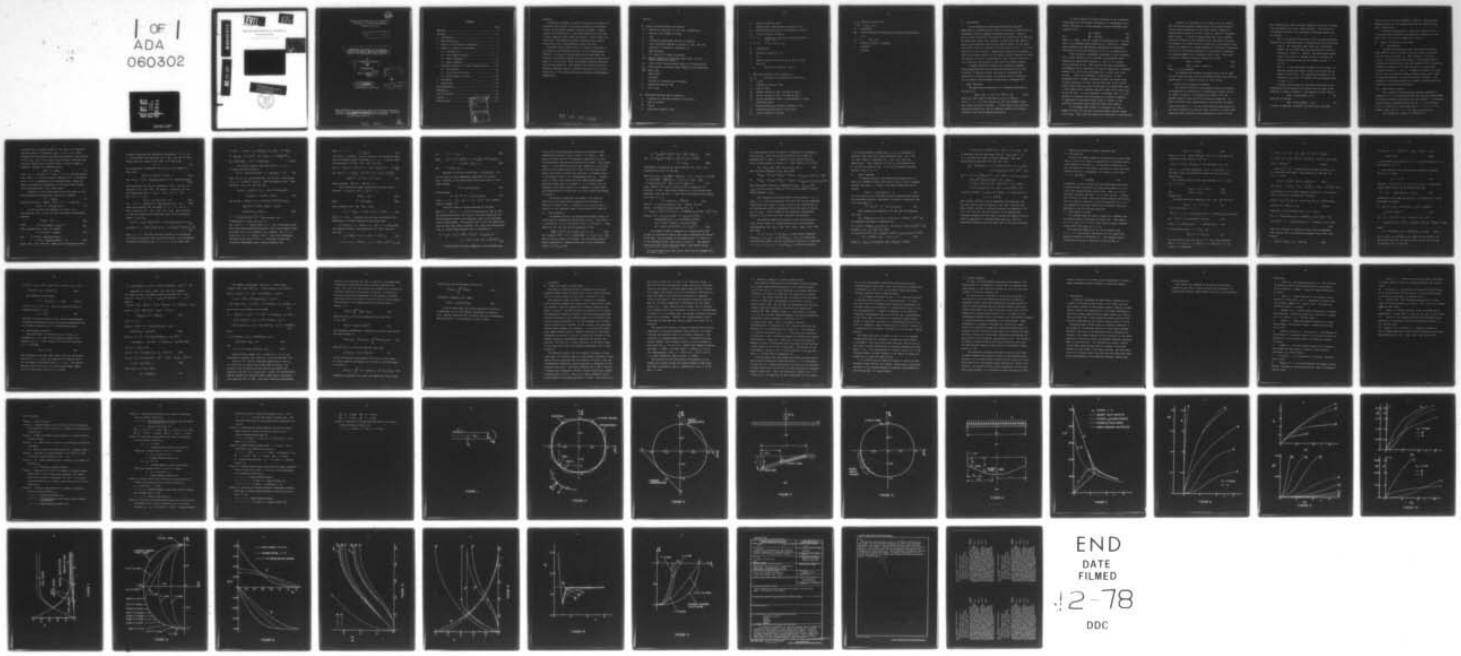

END
DATE
FILMED
12-78
DDC

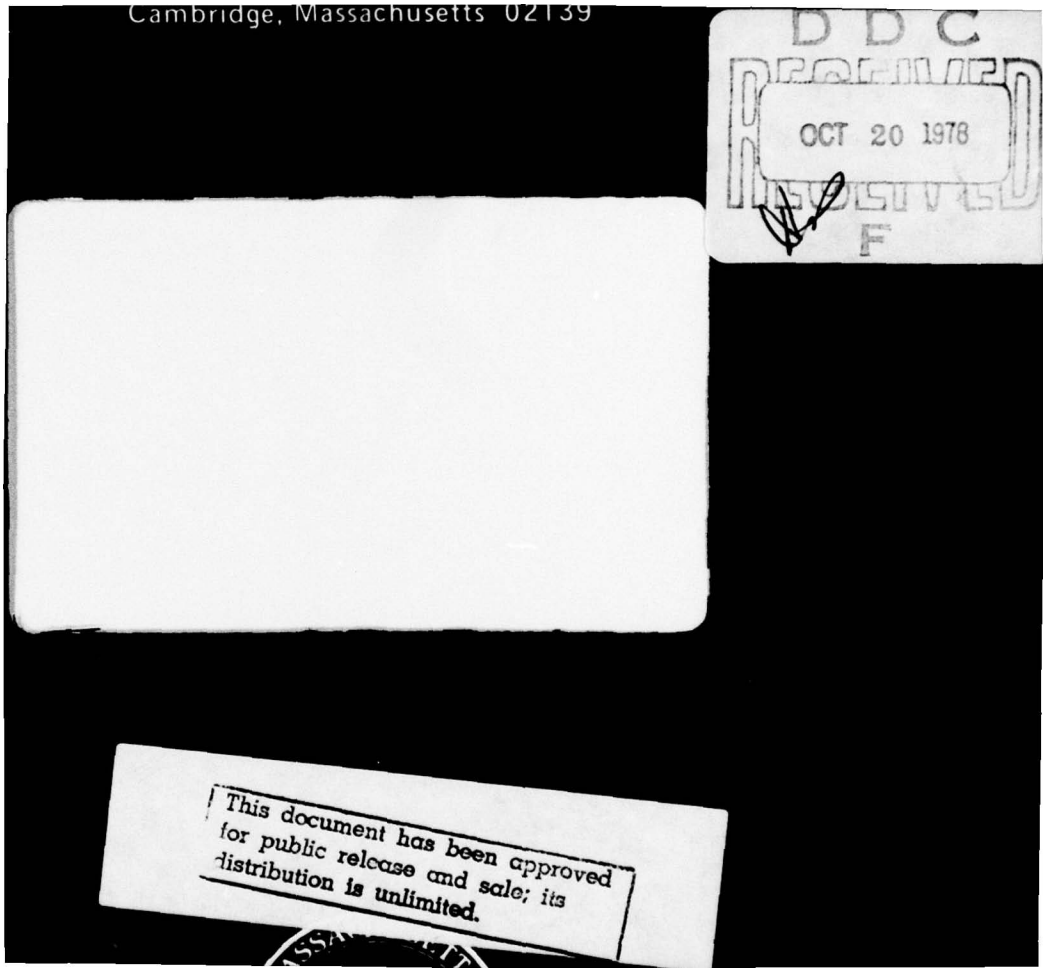
Cambridge, Massachusetts 02139
DDC
OCT 20 1978
F
This document has been approved
for public release and sale; its
distribution is unlimited.

(12)

MASSACHUSETTS INSTITUTE OF TECHNOLOGY
DEPARTMENT OF OCEAN ENGINEERING
CAMBRIDGE, MASS. 02139

(9) Interim rept.,

(6) # A NUMERICAL PROCEDURE FOR THE DYNAMIC PLASTIC RESPONSE OF BEAMS WITH ROTATORY INERTIA AND TRANSVERSE SHEAR EFFECTS.

by

(10) J. Gomes de Oliveira
[redacted]
Norman Jones

Report Number (14) 78-2

(11) Aug[redacted]78

(12) 64p.

Distribution Unlimited

This research was carried out under the Structural Mechanics Program of the Office of Naval Research, Arlington, Virginia. Contract number (15) N00014-76-C-0195, Task NR 064-510.

406 856

CONTENTS

page

Abstract..... i

Notation.....ii

1. Introduction..... 1

2. Basic Equations..... 1

3. Details of the Numerical Procedure..... 3

4. Impact of a Mass on a Long Beam..... 5

4.1 Introduction..... 5

4.2 First Phase of Motion..... 5

4.3 Type A Response.....11

4.4 Type B Response.....14

5. Impulsive Loading of a Simply Supported Beam.....16

5.1 Introduction.....16

5.2 First Phase of Motion.....16

5.3 Second Phase of Motion.....20

6. Discussion.....25

7. Conclusions.....30

Acknowledgements.....31

References.....32

List of Figures.....34

Figures.....38

Library Card.....55

Abstract

A numerical procedure is used to examine the influence of transverse shear forces in the yield criterion and rotatory inertia on the dynamic plastic response of beams. Various results are presented for a long beam impacted by a mass and a simply supported beam loaded impulsively, both of which are made from a rigid perfectly plastic material with yielding controlled by the Ilyushin-Shapiro yield criterion.

Transverse shear effects lead to a dramatic reduction in the slopes of the deformed profiles for both beam problems. Moreover, the slope of the deformed profile underneath the striker in the impact problem is quite sensitive to the actual shape of a yield curve, while the maximum transverse displacement is less sensitive. The retention of rotatory inertia in the basic equations leads to further reductions up to 17 and 10 per cent in the slopes and maximum transverse displacements, respectively.

Notation

(a) Notation used throughout the article

e, f defined by equations (6) and (17f), respectively.

m mass per unit length of a beam

t time

w transverse displacement defined in Figure 1.

x axial coordinate defined in Figures 1, 4(b), and 6(b).

z location of interface in equations (2)

H beam thickness

I_r mk^2, where k is radius of gyration

M,Q bending moment and transverse shear force (per unit length) defined in Figure 1

M_o fully plastic bending moment capacity of cross-section

Q_o fully plastic transverse shear capacity of cross-section

$\bar{M},\bar{Q}$ M/M_o, Q/Q_o

γ shear angle

κ curvature

ψ rotation of mid-plane due to bending

Ω defined by equation (9b)

$(\dot{})$ $\partial/\partial t$, $\partial/\partial T$.

(b) Additional Notation used in Section 4

z location of interface defined in Figure 4(b).

G mass of striker

I^2 mI_r/G^2

K defined by equation (17g)

R energy divided by $GV_o^2/2$

T dimensionless time defined by equation (17i)

T_1 dimensionless duration of first phase of motion

V_o initial velocity of mass G

V', V, V_2 transverse velocities of beam defined in Figure 4(b).

$\bar{V}'$, $\bar{V}$, $\bar{V}_2$ V'/V_o, V/V_o, V_2/V_o.

$\bar{W}$ $12mM_o w/G^2V_o^2$.

$\dot{\bar{V}}_2$ defined by equation (17j)

α x/z

θ angular rotation at centre of one half of beam

$\bar{\theta}$ $6M_o\theta/GV_o^2$

λ, λ_o defined by equations (17b, c)

(c) Additional Notation used in Section 5

z_1, z_2 locations of interfaces in Figure 6(b).

I^2 I_r/mL^2

K defined by equation (54d)

$2L$ span of beam

R_B bending energy at time t divided by mLV_o^2

R_K kinetic energy at time t divided by mLV_o^2

R_S energy absorbed in shearing deformations at time t divided by mLV_o^2

T dimensionless time defined by equation (54j)

T_1 dimensionless duration of first phase

V_o initial impulsive velocity

V, V_1 defined in Figure 6(b)

$\bar{V}$, $\bar{V}_1$ V/V_o, V_1/V_o

$\bar{w}$ $M_o w/mL^2 V_o^2$

$\bar{w}_T$ maximum permanent dimensionless transverse displacement

α x/z_1

β_1, β_2 z_1/L, z_2/L

θ angular rotation at supports

$\bar{\theta}$ $M_o \theta/mLV_o^2$

ν $Q_o L/2M_o$

1. Introduction

It was remarked in References [1] and [2] that the importance of transverse shear effects has recently become evident in the dynamic plastic response of various structures. However, the available theoretical solutions on the dynamic plastic behavior of beams which retain the influence of transverse shear employ a square yield condition relating the bending moment (M) and transverse shear force (Q) required for plastic flow [1,3,4]. It is the objective of this article to examine the influence of transverse shear and rotatory inertia on the dynamic plastic response of beams, the behavior of which is controlled by more realistic yield criteria relating the transverse shear force and bending moment.

A simple numerical procedure which employs piecewise linear approximations with any desired accuracy for any yield criterion is developed herein, and used to reconsider the influence of transverse shear and rotatory inertia effects on the two dynamic beam problems investigated in Reference [1].

2. Basic Equations

The equilibrium equations for a Timoshenko beam may be written [1,3]

$$\partial Q/\partial x = m\ddot{w} - q \quad \text{and} \quad Q + \partial M/\partial x = I_r\ddot{\psi} \qquad \text{(1a,b)}$$

where the total slope of the centre line of a beam is $\partial w/\partial x = \psi + \gamma$, ψ is the rotation of the line elements along the centre line due to bending, γ is the shear angle of points along the centre line, and the remaining symbols are defined in Figure 1 and the accompanying Notation.

It may be shown [1,3] that continuity of the transverse displacement (w) and angular deformation (ψ) associated with a moving interface in a rigid perfectly plastic Timoshenko beam requires [1,3]

$$[Q] = m\dot{z}^2[\gamma] \tag{2a}$$

and

$$[M] = I_r\dot{z}^2[\kappa], \tag{2b}$$

where $\kappa = \partial\psi/\partial x$, and $[X]$ means the difference of X on either side of an interface which travels with a velocity $\dot{z}$. Various other kinematic and equilibrium requirements at travelling interfaces are given by equations (3) to (5) in Reference [1].

There has been considerable discussion in the literature and no clear resolution as to whether an interaction curve relating the generalised stresses M and Q is a proper yield criterion or not. This question has been reconsidered in Reference [5] by examining all previous objections, including Heyman's [6], and it was concluded that a yield curve could be used within the framework of beam theory. It was suggested that a suitable compromise between the simple local (stress resultant) and more rigorous non-local (plane stress, plane strain) theories might be achieved for I-beams when using a local theory with a maximum transverse shear force based only on the web area. If this viewpoint is accepted, then it is not possible to describe the local behavior of beams at supports, or underneath concentrated loads, which is similar to the prevailing situation with classical elastic beam theory.

It is evident from Figure 5 in Reference [5] that a number of local and non-local theories predict similar curves in the M/M_o - Q/Q_o plane for beams with rectangular cross-sections.

Ilyushin [7] developed a yield surface for thin shells with solid cross-sections using the von Mises yield criterion and the usual assumptions of thin shell theory. Shapiro [8] extended this theoretical work in order to cater for transverse shear effects. It might be demonstrated when using standard relations between inverse hyperbolic and logarithmic functions that Hodge's [9] yield curve for a beam with a rectangular cross-section is identical to Ilyushin-Shapiro's theoretical predictions [7,8,10] for the plastic yielding of a beam which is subjected to a bending moment and a transverse shear force. This yield criterion is drawn in Figure 2 and may be written

$$Q/Q_o = \phi/\sinh\phi \tag{3a}$$

and

$$M/M_o = \coth\phi - \phi\sinh^{-2}\phi \tag{3b}$$

where ϕ is a parameter.

The theoretical procedure developed herein may be used for any yield criterion, but the Ilyushin-Shapiro yield criterion (equations(3)) is regarded as exact in this article.

3. Details of the Numerical Procedure

The yield criterion in the proposed numerical procedure is replaced by an inscribing or circumscribing polygon having "n" sides, or facets, as illustrated in Figure 2 for the Ilyushin-Shapiro yield criterion governed by equations (3). These piecewise linear approximations coincide with the exact yield curve when $n \to \infty$. It is evident from the corollaries of the limit theorems of plasticity that the static collapse loads associated with inscribing and circumscribing yield criteria

are, respectively, lower and upper bounds to the static collapse load according to the exact yield condition. The choice of n is therefore related to the acceptable difference between the two bounds.

Now it is apparent from Figure 2 that two types of plastic deformation are associated with a piecewise linear yield condition:

Type A. The transverse shear force (Q_i) and bending moment (M_i) are known when the generalised stresses are located at a node "i". However, the generalised plastic strain rate vector is unknown but must lie within the normals associated with the two adjacent facets "i - 1" and "i".

Type B. If the generalised stresses lie on a facet "i", then the generalised plastic strain rate vector must be normal to this facet. The generalised stresses can lie anywhere on the facet "i" between the two adjacent nodes "i" and "i + 1".

A secant linearisation of the exact yield curve is now constructed for the straight line which cuts the exact yield condition as shown in Figure 3. The equation of this line is

$$Q/Q_o + (b_s/a_s)(M/M_o) = b_s \ , \qquad (4)$$

which may be written

$$Q/Q_o \pm (b_s/a_s)(M/M_o) = \pm b_s \qquad (5)$$

in order to describe a straight line which cuts the yield

curve in any of the four quadrants, where a_s and b_s are the absolute values of the intersections with the M/M_o and Q/Q_o axes, respectively.

A tangent linearisation of the exact yield curve is constructed using straight lines which are tangential to the exact yield criterion as indicated in Figure 3.

4. Impact of a Mass on a Long Beam

4.1 Introduction

Consider the infinitely long rigid perfectly plastic beam shown in Figure 4a which is hit by a mass G travelling with an initial velocity V_o. The influence of rotatory inertia and transverse shear forces on the dynamic plastic response of this particular beam was examined from an analytical viewpoint in Reference [1] with the aid of a square yield condition relating Q and M. A numerical solution is sought in this section using the Ilyushin-Shapiro yield curve, which is given by equations (3) and illustrated in Figure 2. The response of this beam consists of a number of phases which are described in the following sections.

4.2 First Phase of Motion

Now, guided by the analytical solution presented in Reference [1], it is conjectured that the velocity profile shown in Figure 4b governs the behavior of this problem. A stationary hinge develops underneath the striker at $x = 0$, the region $0 \leq x \leq z$ rotates as a rigid body, while $z \leq x \leq z + \ell$ is a plastic zone, and $x > z + \ell$ is rigid and stationary.

The theoretical results in Reference [1]

indicate that the bending moment is M_o and Q is negative and quite small in the plastic zone $z \leq x \leq z + \ell$. This suggests that the plastic zone might be confined to the vicinity of the M/M_o axis of the yield curve in Figure 2 and that the piecewise linear yield condition shown in Figure 5 might be adequate. Equation (5) therefore gives

$$M/M_o = 1 + eQ/Q_o \tag{6}$$

since $a_s = 1$ and where $e = 1/b_s$. If $e = 0$, then the tangent line $M/M_o = 1$, which was used in Reference [1], is recovered, while $e > 0$ corresponds to an inscribed facet. These two cases would bound the predictions of the exact yield surface quite accurately when Q/Q_o remains small.

Normality of the generalised strain rate vector to the yield condition represented by equation (6) requires

$$\dot{\gamma}/\dot{\kappa} = -eM_o/Q_o \tag{7}$$

which may be used to express $\partial\dot{w}/\partial x = \dot{\psi} + \dot{\gamma}$ in the form

$$\partial\dot{w}/\partial x = \dot{\psi} - e(M_o/Q_o)\,\partial\dot{\psi}/\partial x \ . \tag{8}$$

It may be shown that equation (1a) with $q = 0$ and equations (1b), (6) and (8) give the partial differential equation

$$\partial^2\ddot{\psi}/\partial x^2 - \Omega^2\ddot{\psi} = 0 \ , \tag{9a}$$

where

$$\Omega^2 = mQ_o^2(me^2M_o^2 + I_rQ_o^2)^{-1} \ . \tag{9b}$$

Thus, equations (9a) and (8) predict

$$\ddot{\psi} = B\sinh\Omega x + C\cosh\Omega x \tag{10}$$

and

$$\ddot{w} = \Omega^{-1}(B - eM_o\Omega C/Q_o)\cosh\Omega x + \Omega^{-1}(C - eM_o\Omega B/Q_o)\sinh\Omega x + D \ , \tag{11}$$

where $B(t)$, $C(t)$, and $D(t)$ remain to be evaluated from the

boundary conditions and continuity requirements. If Q and M are evaluated from equations (1a), (1b), (10) and (11) and substituted into equation (6), then it is found that

$$D = 0 \ . \tag{12}$$

Now integration of equations (10) and (11) with respect to time gives

$$\dot{\psi}(x,t) = E\sinh\Omega x + F\cosh\Omega x \tag{13a}$$

and $$\dot{w}(x,t) = \Omega^{-1}(E - eM_o\Omega F/Q_o)\cosh\Omega x + \Omega^{-1}(F - eM_o\Omega E/Q_o)\sinh\Omega x \tag{13b}$$

when satisfying the initial conditions $\dot{\psi}(x,0) = \dot{w}(x,0) = 0$, and where $E(t)$ and $F(t)$ are unknown. Equations (13) and the requirements $\dot{w}(z,t) = V_2(t)$, $\dot{w}(z + \ell,t) = 0$ and $\dot{\psi}(z + \ell,t) = 0$ give

$$\dot{w}(x,t) = V_2 \exp.\{-\Omega(x - z)\} \tag{14a}$$

and $$\dot{\psi}(x,t) = -(mV_2/I_r\Omega)(1 - eM_o\Omega/Q_o)\exp.\{-\Omega(x - z)\} \ , \tag{14b}$$

when using equation (9b) and where $z \leq x \leq z + \ell$ and $\ell \to \infty$. Thus, equations (1a), (1b), (14a) and (14b) may be solved to give the dimensionless transverse shear force and bending moment in the form

$$\bar{Q}(\alpha,T) = -2\lambda_o K^{-1}\dot{\bar{V}}_2\exp.\{K\lambda(1 - \alpha)\} - 2\lambda_o\bar{V}_2\dot{\lambda}\exp.\{K\lambda(1 - \alpha)\} \tag{15}$$

and $$\bar{M}(\alpha,T) = 1 - 12fK^{-2}\dot{\bar{V}}_2\exp.\{K\lambda(1 - \alpha)\} - 12\bar{V}_2\dot{\lambda}fK^{-1}\exp.\{K\lambda(1 - \alpha)\} \tag{16}$$

when $1 \leq \alpha \leq \infty$ and where the two "constants" of integration are found by requiring that the yield condition (6) is satisfied throughout the plastic zone $(1 \leq \alpha \leq \infty)$ at all times, and

$\alpha = x/z$, $\lambda = mz/G$, $\lambda_o = 6mM_o/Q_oG$, $\bar{Q} = Q/Q_o$, $\bar{M} = M/M_o$,

$f = eM_o\Omega/Q_o$, $K = \Omega G/m$, $\bar{V}_2 = V_2/V_o$, $T = 12mM_ot/G^2V_o$,

$\dot{\bar{V}}_2 = \dot{V}_2G^2/12mM_o$, and $\dot{\lambda} = GV_o\dot{z}/12M_o$. (17a-k)

The velocity field in the rigid region $0 \leq x \leq z$ is linear and may be written

$$\dot{w}(x,t) = (mV_2/I_r\Omega)\{I_r\Omega/m + (1 - eM_o\Omega/Q_o)(z - x)\} \quad (18)$$

when $\dot{w}(z,t) = V_2$ and noting that $\partial\dot{w}(z,t)/\partial x$ in the region $0 \leq x \leq z$ is equal† to $\dot{\psi}(z,t)$ given by equation (14b). Thus, equations (1a), (1b) and (18) give

$$\bar{Q}(\alpha,T) = 2\lambda_o\dot{\bar{V}}_2\{(1 - f)(1 - \alpha/2)\alpha\lambda^2 + I^2K\lambda\alpha\}/I^2K +$$

$$+ 2\lambda_o\bar{V}_2\lambda\dot{\lambda}(1 - f)\alpha/I^2K + \bar{Q}(0,T) \quad (19)$$

and $\bar{M}(\alpha,T) = -12\dot{\bar{V}}_2\{(1 - f)(1 - \alpha/3)\lambda^3\alpha^2/2 + I^2K\alpha^2\lambda^2/2\}/I^2K -$

$$- 6\bar{V}_2\dot{\lambda}\alpha^2\lambda^2(1 - f)/I^2K - 12\dot{\bar{V}}_2(1 - f)\alpha\lambda/K -$$

$$- 6\alpha\lambda\bar{Q}(0,T)/\lambda_o + \bar{M}(0,T), \quad (20)$$

---

† If $[\partial w(z,t)/\partial t] = 0$, then equation (5a) of Reference [1] gives $[Q(z,t)] = 0$. Now $[Q(z,t)] = 0$ implies $[M(z,t)] = 0$ for a non-linear yield curve when disregarding the possibility that M has opposite signs on either side of an interface. Thus, equation (5b) of [1] gives $[\dot{\psi}(z,t)] = 0$. Finally, $\dot{\psi}(x,t) = \partial\dot{w}(x,t)/\partial x$ throughout the rigid region since $\dot{\gamma}(x,t) = 0$, from which follows the continuity requirement used to obtain equation (18).

where $0 \leq \alpha \leq 1$,

$$I^2 = mI_r/G^2 \ , \tag{21}$$

and $\bar{Q}(0,T)$ and $\bar{M}(0,T)$ are the values of the transverse shear force and bending moment evaluated at $x = 0$. It may be shown that equations (15), (16), (19) and (20) give

$$\bar{Q}(0,T) = -\dot{\bar{V}}_2\lambda_o\{(1-f)\lambda^2/I^2K + 2\lambda + 2/K\} - 2\lambda_o\bar{V}_2\dot{\lambda}\{1 + (1-f)\lambda/I^2K\} \tag{22}$$

$$\text{and } \bar{M}(0,T) = 1 - 2\dot{\bar{V}}_2\left\{(1-f)\lambda^3/I^2K + 3\lambda^2 + 6f\lambda/K + 6f/K^2\right\} -$$

$$-6\bar{V}_2\dot{\lambda}\{(1-f)\lambda^2/I^2K + 2\lambda + 2f/K\} \tag{23}$$

when satisfying $[\bar{Q}(1,T)] = [\bar{M}(1,T)] = 0$.

Now, equilibrium under the striker travelling with a velocity V' requires $Q(0,t) = G\dot{V}'/2$, or

$$\bar{Q}(0,T) = \lambda_o\dot{\bar{V}}' \ , \tag{24a}$$

where

$$\dot{\bar{V}}' = G^2\dot{V}'/12mM_o \ . \tag{24b}$$

Thus, equations (22) and (24a) yield

$$\bar{V}' = 1 - 2\bar{V}_2\{(1-f)\lambda^2/2 + I^2K\lambda + I^2\}/I^2K, \tag{25}$$

where $\bar{V}' = V'/V_o$. Equation (25) may also be obtained from conservation of linear momentum of the entire beam.

If $\bar{Q}(0,T) = -1$, $\bar{M}(0,T) = 0$, and $\dot{\lambda} = 0$ during the first phase of motion, then equations (18), (22), (23), and (25) give

$$\bar{V}_2 = I^2KT\{(1-f)\lambda_1^2 + 2I^2K\lambda_1 + 2I^2\}^{-1}/\lambda_o \tag{26}$$

$$\bar{V} = \{(1-f)\lambda_1 + I^2K\}T\{(1-f)\lambda_1^2 + 2I^2K\lambda_1 + 2I^2\}^{-1}/\lambda_o \tag{27}$$

and $\bar{V}' = 1 - T/\lambda_o$, (28)

where $2(1 - f)\lambda_1^3 + \{6I^2K - (1 - f)\lambda_o\}\lambda_1^2 + 2I^2(6f - K\lambda_o)\lambda_1 +$

$+ 12fI^2/K - 2I^2\lambda_o = 0$, (29)

and $\bar{V} = \dot{w}(0,t)/V_o$.

Equation (5) can be written $Q/Q_o + (b_1/a_1)(M/M_o) = -b_1$ for the plastic hinge immediately underneath the striker. Thus, normality of the generalised strain rate vector to this facet demands

$$\dot{\kappa}/\dot{\gamma} = (b_1/a_1)(Q_o/M_o) \tag{30}$$

which becomes

$$(\bar{V} - \bar{V}_2)/(\bar{V}' - \bar{V}) = (6\lambda_1/\lambda_o)(b_1/a_1) \tag{31}$$

since $\dot{\gamma} = -(V' - V)/\ell$ and $\dot{\kappa} = -(V - V_2)/z\ell$ for a plastic hinge of length "ℓ".

The first phase of motion continues at the node $\bar{M}(0,T) = 0$, $\bar{Q}(0,T) = -1$ until the dimensionless time T_1 when the generalised strain rate vector in the beam underneath the striker becomes normal to the adjacent facet of the piecewise linear yield surface. If equations (26) to (28) are substituted into the left hand side of equation (31), then the dimensionless time T_1 occurs when equation (31) is satisfied, or

$$T_1 = \lambda_o\{(1 - f)\lambda_1^2 + 2I^2K\lambda_1 + 2I^2\}\{(1 - f)\lambda_o(a_1/b_1)/6 +$$

$$+ (1 - f)(1 + \lambda_1)\lambda_1 + (2\lambda_1 + 1)I^2K + 2I^2\}^{-1} . \tag{32}$$

A second phase of motion commences at the dimensionless

time T_1 with the generalized stresses at the plastic hinge underneath the striker lying on facet 1 in Figure 5. This phase of motion with $\dot{\lambda} \neq o$ is eventually completed at T_2 when the generalized stresses have migrated along facet 1 and reached node 2. A third phase of motion then commences at T_2 with the generalized stresses remaining at node 2 and the generalized strain rate vector rotating with time until it becomes normal to the adjacent facet 2 at a dimensionless time T_3. A fourth stage of motion then follows with the generalized stresses migrating along facet 2 in Figure 5. It is evident that the response of this beam consists of a sequence of phases which are characterized as either type A or type B which are defined in section 3.

The governing equations are sought in the next two sections for the cases when the generalized stresses are either at a typical node i (type A) or on a typical facet i (type B) of the piecewise linear yield condition in Figure 2.

4.3 Type A Response

As remarked earlier, the generalized stresses remain at a node during a response characterized as type A. Now, $\bar{Q}(O,T) = -d_i$ and $\bar{M}(O,T) = -g_i$ at the typical node "i" in Figure 2. Thus, equations (22) and (23) may be integrated to give

$$\bar{V}_2\left\{(1-f)\lambda^2/I^2K + 2\lambda + 2/K\right\} = d_i\, T/\lambda o + C_1 \qquad (33a)$$

and $$2\bar{V}_2\left\{(1-f)\lambda^3/I^2K + 3\lambda^2 + 6f\lambda/K + 6f/K^2\right\} = (1 + g_i)T + C_2, \qquad (33b)$$

where C_1 and C_2 remain to be found. If the present phase of motion commenced at a dimensionless time T_k with associated values λ_k and $V_{2(k)}$, then

$$C_1 = \bar{V}_{2(k)}\left\{(1-f)\lambda_k^2/I^2K + 2\lambda_k + 2/K\right\} - d_i T_k/\lambda_o \qquad (34a)$$

and $$C_2 = 2\bar{V}_{2(k)}\left\{(1-f)\lambda_k^3/I^2K + 3\lambda_k^2 + 6f\lambda_k/K + 6f/K^2\right\} - \\ - (1 + g_i)T_k. \qquad (34b)$$

Furthermore, eliminating $\bar{V}_2$ from equations (33) gives λ at a dimensionless time T in the form

$$\left\{2(1-f)(d_i T/\lambda_o + C_1)/I^2K\right\}\lambda^3 + \left\{6(d_i T/\lambda_o + C_1) - (1-f)(1 + g_i)T/I^2K \right. \\ \left. -(1-f)C_2/I^2K\right\}\lambda^2 + 2\left\{6f(d_i T/\lambda_o + C_1)/K - (1 + g_i)T - C_2\right\}\lambda \\ + 12f(d_i T/\lambda_o + C_1)/K^2 - 2\left\{(1 + g_i)T + C_2\right\}/K = 0. \qquad (35)$$

Thus, equation (35) with C_1 and C_2 given by equations (34) predicts λ at any T which then allows $\bar{V}_2$ to be calculated using equations (33a) and (34a). $\bar{V}$ may then be evaluated from equation (18) with x = 0, or

$$\bar{V} = \bar{V}_2\left\{(1-f)\lambda + I^2K\right\}/I^2K \qquad (36)$$

while $\bar{V}'$ is given by equation (25). Finally, $\dot{\bar{V}}_2$ and $\dot{\lambda}$ follow by differentiating equations (33), or

$$\dot{\lambda} = \left[d_i/\lambda_o - \dot{\bar{V}}_2\left\{(1-f)\lambda^2/I^2K + 2\lambda + 2/K\right\}\right]\left[2\bar{V}_2\left\{(1-f)\lambda/I^2K + 1\right\}\right]^{-1}, \qquad (37a)$$

and $$\dot{\bar{V}}_2 = \left[(1 + g_i)\lambda_o\left\{(1-f)\lambda/I^2K + 1\right\} - 3d_i\left\{(1-f)\lambda^2/I^2K + \right.\right. \\ \left.\left. +2\lambda + 2f/K\right\}\right]\left[2\lambda_o\left\{1 + (1-f)\lambda/I^2K\right\}\left\{(1-f)\lambda^3/I^2K + \right.\right. \\ \left.\left. +3\lambda^2 + 6f\lambda/K + 6f/K^2\right\} - 3\lambda_o\left\{(1-f)\lambda^2/I^2K + \right.\right. \\ \left.\left. +2\lambda + 2f/K\right\}\left\{(1-f)\lambda^2/I^2K + 2\lambda + 2/K\right\}\right]^{-1}. \qquad (37b)$$

This phase of motion commences at a dimensionless time T_k when the generalized strain rate vector underneath the striker is at node i and is assumed to be perpendicular † to facet i-1 of the piecewise linear yield curve in Figure 2. The generalized strain rate vector remains at node i and rotates during

---

† The generalized strain rate vector could also be perpendicular to facet i at T_k.

the ensuing motion until the phase is completed at a dimensionless time T_{k+1}, when the generalized strain rate vector is perpendicular to facet i or returns to its initial position, which is perpendicular to facet i-1. Thus, equation (31) gives

$$(\bar{V}_k - \bar{V}_{2(k)})(\bar{V}_k' - \bar{V}_K) = (6\lambda_k/\lambda_o)(b_{i-1}/a_{i-1}) \qquad (38a)$$

when the phase commences at T_k, and either

$$(\bar{V}_{(k+1)} - \bar{V}_{2(k+1)})/(\bar{V}'_{(k+1)} - \bar{V}_{(k+1)}) = (6\lambda_{(k+1)}/\lambda_o)(b_i/a_i), \qquad (38b)$$

or

$$(\bar{V}_{(k+1)} - \bar{V}_{2(k+1)})/(\bar{V}'_{(k+1)} - \bar{V}_{(k+1)}) = (6\lambda_{(k+1)}/\lambda_o)(b_{i-1}/a_{i-1}) \qquad (38c)$$

when this phase of motion is completed at T_{k+1}. $V_{2(k+1)}$ and $\lambda_{(k+1)}$ are the initial values for the following phase of motion which commences at T_{k+1}.

The transverse velocities within the two zones $o \leq x \leq z$ and $z \leq x \leq \infty$ given by equations (18) and (14a) may be integrated numerically with respect to time to predict the contribution to the displacement profile accumulated during the phase of motion $T_k \leq T \leq T_{k+1}$. This is added to the transverse displacement profile at T_k to give the total transverse displacement.

The bending moment and transverse shear force distributions in both zones at a dimensionless time T are calculated from equations (15), (16), (19), (20), (33a), (34a), (35), (37a) and (37b).

If $k = 0$, $T_o = 0$, and $\bar{V}_{2(o)} = 0$ when motion commences, then $T_{k+1} = T_1$, $\lambda_{k+1} = \lambda_1$, and $\bar{V}_{2(k+1)} = \bar{V}_{2(1)}$ are associated with the first phase of motion considered in section 4.2 provided $i = 1$, $d_i = 1$, $g_i = 0$, $\dot{\lambda} = 0$, and $\bar{V}_{2(1)}$ is identified with $\bar{V}_2$.

It is straightforward to show that $C_1 = C_2 = 0$ according to equations (34a) and (34b), while equations (33a), (35), (36), and (38b) reduce to equations (26), (29), (27), and (31), respectively. Thus, equation (32) for T_1 is recovered since $\bar{V}'$ is given by equation (25). It is not necessary to satisfy equation (38a) at $T_o = 0$.

4.4 Type B Response

As remarked earlier, the generalized stresses lie on a facet of a piecewise linear yield curve during a type B response. Consider the facet i in Figure 2 for which equation(5) may be written

$$\bar{Q}(0,T) + (b_i/a_i)\bar{M}(0,T) = -b_i \qquad (39)$$

for the plastic flow in the beam directly underneath the striker. The associated normality requirement according to equations (30), (31), and (38b) is

$$(\bar{V} - \bar{V}_2)/(\bar{V}' - \bar{V}) = (6\lambda/\lambda_o)(b_i/a_i). \qquad (40)$$

Now, substituting equations (25) and (36) into equation (40) gives

$$\bar{V}_2 = I^2K\{(a_i/b_i)(1-f)\lambda_o/6 + (1-f)(1+\lambda)\lambda + I^2K(1+2\lambda) + 2I^2\}^{-1} \qquad (41)$$

and therefore according to equation (36)

$$\bar{V} = \{(1-f)\lambda + I^2K\}\{(a_i/b_i)(1-f)\lambda_o/6 + (1-f)(1+\lambda)\lambda + I^2K(1+2\lambda)+2I^2\}^{-1}. \qquad (42)$$

Equations (22), (23) and (39) yield

$$T = \bar{V}_2 [2(1-f)\lambda^3/I^2K + 6\lambda^2 + 12f\lambda/K + 12f/K^2 + (a_i/b_i)\lambda_o\{(1-f)\lambda^2/I^2K + 2\lambda + 2/K\}](1 + a_i)^{-1} - C_1(1 + a_i)^{-1}, \qquad (43)$$

where $C_1 = \bar{V}_{2(k)} [2(1-f)\lambda_k^3/I^2K + 6\lambda_k^2 + 12f\lambda_k/K + 12f/K^2 +$

$$+ (a_i/b_i)\lambda_o \{(1-f)\lambda_k^2/I^2K + 2\lambda_k + 2/K\}\,] - (1 + a_i)T_k \qquad (44)$$

is obtained from the requirement that $\bar{V}_2 = \bar{V}_{2(k)}$ and $\lambda = \lambda_k$ at $T = T_k$ when this phase of motion commences. The time derivatives of equations (41) and (43) give

$$\dot{\bar{V}}_2 = -I^2K\dot{\lambda}\{2(1-f)\lambda + 1-f + 2I^2K\}\{(1-f)\lambda^2 + (1-f + 2I^2K)\lambda + \\ + (1-f)\lambda_o(a_i/b_i)/6 + I^2K + 2I^2\}^{-2} \qquad (45)$$

and

$$\dot{\lambda} = \{(1 + a_i)/I^2K\}\{(1-f)\lambda^2 + (1-f + 2I^2K)\lambda + (1-f)\lambda_o(a_i/b_i)/6 + \\ + I^2K + 2I^2\}^2 / \Big[[6(1-f)\lambda^2/I^2K + 12\lambda + 12f/K + \\ + (a_i/b_i)\lambda_o\{2(1-f)\lambda/I^2K + 2\}]\{(1-f)\lambda^2 + (1-f + 2I^2K)\lambda + \\ + (1-f)\lambda_o(a_i/b_i)/6 + I^2K + 2I^2\} - [2(1-f)\lambda^3/I^2K + 6\lambda^2 + \\ + 12f\lambda/K + 12f/K^2 + \lambda_o(a_i/b_i)\{(1-f)\lambda^2/I^2K + 2\lambda + 2/K\}]\{2(1-f)\lambda + \\ + 1 - f + 2I^2K\}\Big]. \qquad (46)$$

Thus, $\bar{Q}(0,T)$ and $\bar{M}(0,T)$ may be evaluated from equations (22) and (23) with the aid of equations (41), (43), (45) and (46). Hence, $\bar{Q}(\alpha,T)$ and $\bar{M}(\alpha,T)$ may be calculated from equations (15), (16), (19) and (20) and the migration of the generalized stresses followed along the facet i during this phase of motion, which is completed at a dimensionless time T_{k+1}, when the generalized stresses reach the next node i+1 or return to node i.

5. Impulsive Loading of a Simply Supported Beam

5.1 Introduction

Consider the simply supported rigid perfectly plastic beam shown in Figure 6(a) which is subjected to a uniformly distributed impulsive velocity V_o. It was found in Reference [1] that the behavior of this beam is governed by transverse shear effects alone and is independent of rotatory inertia when $0 \leq \nu \leq 1$ and where

$$\nu = Q_o L/2M_o. \tag{47}$$

Furthermore, it may be shown that the associated generalised stresses $\bar{M}$ and $\bar{Q}$ throughout the entire beam either lie in or within the Ilyushin-Shapiro yield curve. Thus, it is only required to examine the case $\nu \geq 1$ in this section. A numerical solution is sought using the Ilyushin-Shapiro yield curve, which is given by equations (3) and illustrated in Figure 2. The response of this beam consists of two phases, which are described in the two following sections.

5.2 First Phase of Motion

It is assumed that the beam in Figure 6(a) responds with the velocity field illustrated in Figure 6(b). The regions $0 \leq x \leq z_1$ and $z_2 \leq x \leq L$ are rigid, while a plastic zone develops within the region $z_1 \leq x \leq z_2$.

The transverse shear force (Q) in the plastic zone ($z \leq x \leq L$) is quite small and positive in the theoretical analysis presented in Reference [1]. This suggests that a linearisation similar to equation (6) may be used, or

$$M/M_o = -1 + eQ/Q_o \qquad (48)$$

when $z_1 \leq x \leq z_2$. Thus, equations (10) to (12) are again obtained which give equation (13a) and

$$\dot{w}(x,t) = \Omega^{-1}(E - fF)\cosh\Omega x + \Omega^{-1}(F-fE)\sinh\Omega x + V_o \qquad (49)$$

for $z_1 \leq x \leq z_2$ when satisfying $\dot{\psi}(x,0) = 0$ and $\dot{w}(x,0) = V_o$ and where Ω and f are defined by equations (9b) and (17f), respectively.

The velocity fields in the rigid regions $0 \leq x \leq z_1$ and $z_2 \leq x \leq L$ are

$$\dot{w}(x,t) = C(t) + D(t)x \qquad (50a)$$

and

$$\dot{w}(x,t) = G(t), \qquad (50b)$$

respectively.

It may be shown that equations (13a), (49), and (50) give

$$\dot{\bar{W}}(\alpha,T) = \bar{V}_1 + (\bar{V} - \bar{V}_1)\alpha \qquad (51)$$

in the rigid zone $0 \leq \alpha \leq 1$,

$$\dot{\bar{W}}(\alpha,T) = 1 + (\bar{V} -1)[\cosh\{K(\beta_2-\alpha\beta_1)\} + f\sinh\{K(\beta_2-\alpha\beta_1)\}]/B, \qquad (52a)$$

and

$$\dot{\bar{\psi}}(\alpha,T) = K(1-\bar{V})\sinh\{K(\beta_2-\alpha\beta_1)\}/B, \qquad (52b)$$

where

$$B = \cosh\{K(\beta_2-\beta_1)\} + f\sinh\{K(\beta_2-\beta_1)\} \qquad (52c)$$

in the plastic zone $1 \leq \alpha \leq \beta_2/\beta_1$, and

$$\dot{\bar{W}}(\alpha,T) = 1 + (\bar{V}-1)/B \qquad (53)$$

for the central rigid zone $\beta_2/\beta_1 \leq \alpha \leq 1/\beta_1$, when satisfying $\dot{w}(0,t) = V_1$, $\dot{w}(z_1,t) = V$, $[\dot{w}(z_1,t)] = 0$, $[\dot{w}(z_2,t)] = 0$, and $[\dot{\psi}(z_2,t)] = 0$, and where

$\alpha = x/z_1$, $\beta_1 = z_1/L$, $\beta_2 = z_2/L$, $K = \Omega L$, $I^2 = I_r/mL^2$,

$\bar{V} = V/V_o$, $\bar{V}_1 = V_1/V_o$, $\dot{\bar{W}}(\alpha,t) = \dot{w}(x,t)/V_o$, $\dot{\bar{\psi}}(\alpha,T) = L\dot{\psi}(x,t)/V_o$,

and $T = M_o t/mV_o L^2$. (54a-j)

Now, if $\dot{z}_1 = \dot{z}_2 = 0$ during the first phase of motion (i.e., no travelling interfaces), then equations (1) and (51) for $0 \leq \alpha \leq 1$ give

$$\bar{Q}(\alpha,T) = \alpha^2\beta_1(\dot{\bar{V}} - \dot{\bar{V}}_1)/4\nu + \alpha\beta_1\dot{\bar{V}}_1/2\nu + 1 \quad (55a)$$

and $$\bar{M}(\alpha,T) = \alpha^3\beta_1{}^2(\dot{\bar{V}}_1 - \dot{\bar{V}})/6 - \alpha^2\beta_1{}^2\dot{\bar{V}}_1/2 - 2\alpha\beta_1\nu + \alpha I^2(\dot{\bar{V}}-\dot{\bar{V}}_1) \quad (55b)$$

since $\bar{M}(0,T) = 0$ for simple supports and $\bar{Q}(0,T) = 1$ for plastic flow to develop at the supports, and where

$\bar{Q}(\alpha,T) = Q(x,t)/Q_o$, $\bar{M}(\alpha,t) = M(x,t)/M_o$, $\dot{\bar{V}}(\alpha,t) = mL^2\dot{V}(x,t)/M_o$,

and $\dot{\bar{V}}_1(\alpha,T) = mL^2\dot{V}_1(x,t)/M_o$. (56a-d)

Similarly, for the plastic zone ($1 \leq \alpha \leq \beta_2/\beta_1$),

$$\bar{Q}(\alpha,T) = -\dot{\bar{V}}[\sinh\{K(\beta_2-\alpha\beta_1)\} + f\cosh\{K(\beta_2 -\alpha\beta_1)\}]/2\nu BK \quad (57a)$$

and $$\bar{M}(\alpha,T) = -1 - f\dot{\bar{V}}[\sinh\{K(\beta_2-\alpha\beta_1)\} + f\cosh\{K(\beta_2 -\alpha\beta_1)\}]/BK^2, \quad (57b)$$

where the constants of integration were found by demanding that equation (48) was satisfied throughout the plastic zone. Finally,

$$\bar{Q}(\alpha,T) = \dot{\bar{V}}(\alpha\beta_1 - \beta_2 - f/K)/2\nu B \quad (58a)$$

and $\bar{M}(\alpha,T) = -1 - \dot{\bar{V}}[\alpha^2\beta_1^2/2 - \alpha\beta_1\beta_2 - \alpha f\beta_1/K + 1/2 +$

$+(f/K)^2/2]/B$ (58b)

in the central rigid zone $\beta_2/\beta_1 \leq \alpha \leq 1/\beta_1$ when $[Q(\beta_2/\beta_1,T)] = 0$ and $[M(\beta_2/\beta_1, T)] = 0$.

Thus, equation (58a) satisfies the symmetry requirement $\bar{Q}(1/\beta_1, T) = 0$ when

$$\beta_2 = 1 - f/K. \tag{59}$$

Moreover, $\partial\dot{w}(x,t)/\partial x$ at $x = z_1$ (i.e., $\dot{\psi}(z_1,t)$) in the rigid region equals $\dot{\psi}(z_1,t)$ in the plastic zone when

$$\dot{\bar{V}} - \dot{\bar{V}}_1 = -\beta_1 K\dot{\bar{V}} \sinh\{K(\beta_2 - \beta_1)\}/B. \tag{60}$$

Furthermore, the conditions $[\bar{Q}(1,T)] = 0$ and $[\bar{M}(1,T)] = 0$ may be solved to predict

$$\dot{\bar{V}} = (\nu\beta_1^2/3 - \beta_1/2 - 2I^2\nu)(\beta_1^3/12 + \beta_1 I^2 + \beta_1 fD/2K^2 +$$

$$\beta_1^2 D/3K + I^2 D/K)^{-1} \tag{61a}$$

and $\dot{\bar{V}}_1 = -(2\nu\beta_1^2/3 - \beta_1/2 + 2\nu\beta_1 D/K - D/K + 2I^2\nu +$

$$+2\nu fD/K^2)(\beta_1^3/12 + I^2\beta_1 + f\beta_1 D/2K^2 + D\beta_1^2/3K + I^2 D/K)^{-1}, \tag{61b}$$

where

$$D = [\sinh\{K(\beta_2 - \beta_1)\} + f\cosh\{K(\beta_2 - \beta_1)\}]/B, \tag{61c}$$

and β_1 and β_2 are related to the length of the plastic zone and satisfy equation (60) which can be written with the aid of equations (61) in the form

$$K(\nu\beta_1^2/3 - \beta_1/2 - 2I^2\nu)\sinh\{K(\beta_2 - \beta_1)\}/B = (\beta_1 - \nu\beta_1^2 - 2\nu\beta_1 D/K + D/K - 2\nu f D/K^2)/\beta_1. \quad (62)$$

Now, equations (61) predict

$$\bar{V} = 1 + \dot{\bar{V}}T \text{ and } \bar{V}_1 = 1 + \dot{\bar{V}}_1 T \quad (63a,b)$$

since $\bar{V} = \bar{V}_1 = 1$ at $T = 0$. The first phase of motion is completed when $\bar{V}_1 = 0$, or

$$T_1 = -1/\dot{\bar{V}}_1, \quad (64)$$

where $\dot{\bar{V}}_1$ is given by equation (61b), and the corresponding transverse displacement profile and angular deformations can be evaluated analytically in a straightforward manner.

5.3 Second Phase of Motion

The second phase of motion with $\dot{z}_1 \neq 0$ and $\dot{z}_2 = 0$ commences at $T = T_1$, when plastic shearing ceases at the supports ($V_1 = 0$). Thus, equation (51) for the rigid zone $0 \leq \alpha \leq 1$ becomes

$$\dot{\bar{W}}(\alpha, T) = \dot{\bar{V}}\alpha, \quad (65)$$

while equations (52a) and (52b) remain valid for the plastic zone with $1 \leq \alpha \leq \beta_2/\beta_1$, and equation (53) remains valid for the central rigid region $\beta_2/\beta_1 \leq \alpha \leq 1/\beta_1$. The requirement that $\partial\dot{w}(x,t)/\partial x$ at $x = z_1$ in the rigid region equals $\dot{\psi}(x,t)$ in the plastic zone at $x = z_1$ gives

$$\bar{V} = \beta_1 K \tanh\{K(\beta_2 - \beta_1)\}[1 + (f+\beta_1 K)\tanh\{K(\beta_2 - \beta_1)\}]^{-1}. \quad (66)$$

Equations (1), (52a), (52b), (53), and (65) together with equation (48), the simply supported boundary conditions, $[\bar{Q}(\alpha,T)] = [\bar{M}(\alpha,T)] = 0$ at $\alpha = \beta_2/\beta_1$ and $[\bar{Q}(\alpha,T)] = 0$ at $\alpha = 1$ predict

$$\bar{Q}(\alpha,T) = (\dot{\bar{V}}\dot{\beta}_1 - \ddot{\bar{V}}\beta_1)(1 - \alpha^2)/4\nu - \dot{\bar{V}}D/2\nu K - (\bar{V} - 1)D^2\dot{\beta}_1/2\nu \quad (67a)$$

$$\bar{M}(\alpha,T) = (\dot{\beta}_1\bar{V} - \beta_1\dot{\bar{V}})(\alpha^3\beta_1/6 - \beta_1\alpha/2 - \alpha I^2/\beta_1) +$$

$$+ \dot{\bar{V}}\alpha D\beta_1/K + (\bar{V} - 1)D^2\alpha\beta_1\dot{\beta}_1 \quad (67b)$$

for $0 \le \alpha \le 1$,

$$\bar{Q}(\alpha,T) = -\{\dot{\bar{V}}/K + (\bar{V} - 1)D\dot{\beta}_1\}[\sinh\{K(\beta_2 - \alpha\beta_1)\} +$$

$$+ f\cosh\{K(\beta_2 - \alpha\beta_1)\}]/2\nu B \quad (68a)$$

$$\bar{M}(\alpha,T) = -1 - \{\dot{\bar{V}} + (\bar{V}-1)\dot{\beta}_1 DK\}[\cosh\{K(\beta_2 - \alpha\beta_1)\}/BK^2 +$$

$$+ f\sinh\{K(\beta_2 - \alpha\beta_1)\}/BK^2 - I^2\cosh\{K(\beta_2 - \alpha\beta_1)\}/B] \quad (68b)$$

for $1 \le \alpha \le \beta_2/\beta_1$, and

$$\bar{Q}(\alpha,T) = \{\dot{\bar{V}} + (\bar{V}-1)KD\dot{\beta}_1\}(\alpha\beta_1 - \beta_2 - f/K)/2\nu B \quad (69a)$$

$$\bar{M}(\alpha,T) = \{\dot{\bar{V}} + (\bar{V}-1)KD\dot{\beta}_1\}\{I^2 - 1/K^2 - (\alpha^2\beta_1^2 - 2\alpha\beta_1\beta_2 + \beta_2^2)/2 -$$

$$-f(\beta_2 - \alpha\beta_1)/K\}/B - 1 \quad (69b)$$

when $\beta_2/\beta_1 \le \alpha \le 1/\beta_1$, where

$$\dot{\beta}_1 = mLV_o\dot{z}_1/M_o. \quad (70)$$

The symmetry requirement $\bar{Q}(1/\beta_1,T) = 0$ again gives equation (59), while $[\bar{M}(1,T)] = 0$ with equation (66) predicts

$$\dot{\bar{V}}[\beta_1^2/3 + D\beta_1/K + I^2 + 1/K^2 - I^2 \cosh\{K(\beta_2 - \beta_1)\}/B] -$$

$$- [\beta_1/3 + I^2/\beta_1 + D^2B \operatorname{cosech}\{K(\beta_2 - \beta_1)\}/K +$$

$$+ DB \operatorname{cosech}\{K(\beta_2 - \beta_1)\}/K^2\beta_1 - I^2D \coth\{K(\beta_2 - \beta_1)\}/\beta_1]\bar{V}\dot{\beta}_1 = -1 \quad (71)$$

which again using equation (66) becomes

$$\dot{\beta}_1 = -Q^2\Big[[\beta_1^2/3 + D\beta_1/K + I^2 + 1/K^2 - I^2 \cosh\{K(\beta_2 - \beta_1)\}/B]P -$$

$$- [\beta_1^2 K \tanh\{K(\beta_2 - \beta_1)\}/3 + I^2K \tanh\{K(\beta_2 - \beta_1)\} +$$

$$+ D^2\beta_1 B \operatorname{sech}\{K(\beta_2 - \beta_1)\} + DB \operatorname{sech}\{K(\beta_2 - \beta_1)\}/K - I^2DK]Q\Big]^{-1}, \quad (72)$$

where

$$P = K \tanh\{K(\beta_2 - \beta_1)\} + fK\tanh^2\{K(\beta_2 - \beta_1)\} -$$

$$-\beta_1K^2 \operatorname{sech}^2\{K(\beta_2 - \beta_1)\} \quad (73a)$$

and

$$Q = 1 + (f + \beta_1K) \tanh\{K(\beta_2 - \beta_1)\} . \quad (73b)$$

Motion finally ceases at $T = T_2$ when $\bar{V} = 0$, or $\beta_1 = \beta_2$ according to equation (66), where β_2 is given by equation (59).

Equation (72) must be integrated numerically to give β_1 as a function of T during the second phase of motion. The velocity $\bar{V}$ and acceleration $\dot{\bar{V}}$ may then be calculated from equations (66) and (71), respectively. Hence, the dimensionless bending moments and transverse shear forces may be determined from equations (67) to (69). The total transverse displacement

profile at any position and time is found by a straightforward integration of the velocity field given by equations (51), (52a), (53), and (65) when making due allowance for a travelling interface during the second phase of motion. In particular, the total transverse displacement at the supports is accumulated during the first phase of motion since no further plastic flow develops at the supports during the second phase of motion, i.e.,

$$\bar{W}(0,T) = \int_0^{T_1} \bar{V}_1 dT = T_1/2 \ , \qquad (74)$$

where $\bar{V}_1$ and T_1 are given by equations (63b) and (64), $T \geq T_1$, and

$$\bar{W}(0,T) = M_o w(o,t)/mV_o{}^2L^2. \qquad (75)$$

The transverse displacement accumulated at the mid-span during the second phase is

$$\bar{W}(1/\beta_1,T_2) - \bar{W}(1/\beta_1,T_1) = \int_{T_1}^{T_2} \dot{\bar{W}}(1/\beta_1,T)dT \ , \qquad (76)$$

where $\dot{\bar{W}}(1/\beta_1,T)$ is given by equation (52a), and

$$\bar{W}(1/\beta_1,T_1) = T_1(1 + \dot{\bar{V}}T_1/2B) \qquad (77)$$

is the contribution from equation (53) for the first phase. The total slope at the supports at the end of the first phase of motion is

$$\bar{\theta}(0,T_1) = \int_0^{T_1} (\bar{V} - \bar{V}_1)dT/\beta_1 = (\dot{\bar{V}} - \dot{\bar{V}}_1)T_1{}^2/2\beta_1 \qquad (78)$$

according to equation (51), while the additional slope accumu-

lated during the second phase of motion is

$$\bar{\theta}(0,T_2) = \int_{T_1}^{T_2} \bar{V} dT/\beta_1 \qquad (79)$$

according to equation (65), where

$$\bar{\theta}(0,T) = M_o \theta(0,t)/mLV_o^2. \qquad (80)$$

It may be shown that the various equations in section 4 of Reference [1] for the problem illustrated in Figure 6a with a square yield curve are recovered from the corresponding equations with e = 0 in sections 5.2 and 5.3 here.

6. Discussion

6.1 Impact of a Mass on a Long Beam

The numerical predictions for the response of the rigid perfectly plastic beam in Figure 4(a) hit by a mass travelling with an initial velocity V_o are given in Figures 7 to 12.

The numerical values in Figure 7 indicate a relatively small difference between the results for 2 facets and 50 facets per quadrant, while the results for 10 facets, which are not shown in Figure 7, lie very close to the results for 50 facets. The theoretical results in Figures 7 and 8, with transverse shear retained according to the Ilyushin-Shapiro yield condition but rotatory inertia neglected (I = 0), are compared with the theoretical predictions of Symonds [3] for a square yield condition and the simple bending only solution. It is clear that transverse shear effects lead to a dramatic reduction in the angle underneath the striker ($|\bar{\theta}|$) and a significant increase in the maximum transverse displacement underneath the striker ($\bar{W}$). Moreover, the angle ($\bar{\theta}$) is quite sensitive to the actual shape of the yield curve, while the maximum displacement ($\bar{W}$) is less sensitive.

The numerical results for the combined influence of transverse shear and rotatory inertia on the dynamic response of beams having various cross-sections are compared in Figure 9 with the corresponding theoretical results presented in Reference [1] for a square yield curve. The curves labelled ① to ④ in Figure 9 respectively correspond to W14x87, W12x40, W24x55 wide flanged I-sections and a 3/8 in. wide x 1 in. deep rectangular cross-section beam hit by masses with mH/G = 1.10651. This mass ratio

was used by Parkes [11] in some of his cantilever tests. H was taken as the total depth of a beam, and Q_o was calculated using an area equal to the beam depth times the web thickness and a shear yield stress of $\sigma_o/2$ as discussed in Reference [1]. Again the shape of the yield curve exercises an important effect on the angle $\bar{\theta}$, while the maximum transverse displacement ($\bar{W}$) is fairly insensitive, particularly for the larger values of λ_o. Thus, Figures 8 and 9 suggest that an analysis with a square yield curve (Reference [1] when $I \neq 0$ and Reference [3] when $I = 0$) is adequate when the maximum transverse displacements are of interest. However, the Ilyushin-Shapiro yield curve must be used when the rotation under the striker ($\bar{\theta}$) is required.

The theoretical results in Figure 10 indicate the relative importance of retaining transverse shear forces in the yield criterion and rotatory inertia in the basic equations. The influence of transverse shear forces is consistent with the earlier remarks, while rotatory inertia is not noticeable in the curves for $\lambda_o = 24.357$ (e.g., W14x87 wide flanged I-section with mH/G = 1.10651), but does lead to a reduction in $\bar{\theta}$ of 10%, approximately, when $\lambda_o = 3.31953$ (e.g., 3/8 in. wide x 1 in. deep rectangular beam with mH/G = 1.10651).

The partition of the total energy and migration of the generalised stresses around the Ilyushin-Shapiro yield curve are shown in Figures 11 and 12, respectively, for $\lambda_o = 8.102$ and $I = 0.4276$.

6.2 Impulsive Loading of a Simply Supported Beam

The numerical predictions for the dynamic plastic response of a simply supported beam governed by the Ilyushin-Shapiro yield curve with e = 0.06 and subjected to a uniform impulsive velocity V_o as shown in Figure 6(a) are presented in Figures 13 to 17. The curves labelled ① in Figures 14 and 16 correspond to a beam with a rectangular cross-section, and the curves labelled ②, ③, and ④ are associated with the wide-flanged I-sections having the cross-sections respectively labelled ③, ②, and ① in Figure 9. The results in Figures 13 to 16 are virtually indistinguishable from the corresponding theoretical values presented in Reference [1] for a square yield curve. Thus, the simpler theoretical predictions in Reference [1] for a square yield curve are adequate for the problem shown in Figure 6(a). The presence of a central rigid zone $\beta_2/\beta_1 \leq \alpha \leq 1/\beta_1$ which was considered in sections 5.2 and 5.3 does not appear to influence the results significantly. Indeed $\beta_2 = 0.985$ for the particular beam examined in Figure 17 which means that the central rigid zone has a total width of only 0.03L in this case. The duration of the first phase of motion is $T_1 = 0.10765$ which is to be compared with $T_1 = 0.10795$ found in Reference [1].

It may be shown that the generalised stress profiles associated with the theoretical solutions having I = 0 in References [1] and [4] for a square yield curve, lie within or on Robinson's circular yield curve [5,10] which in turn inscribes the Ilyushin-Shapiro yield curve. Thus, the theoretical results with I = 0 in section 4.1 of Reference [4] and in Reference [1] are identi-

cal to the corresponding theoretical predictions using an Ilyushin-Shapiro yield curve, while the theoretical predictions in Reference [1] with $I \neq 0$ are virtually indistinguishable from the numerical results obtained herein.

It is evident from Figure 14 for $\nu = 1.5$ that the retention of transverse shear effects in an analysis with $I = 0$ gives the same values of $\overline{W}$ (dimensionless transverse displacement at mid-span) which are predicted by a simple bending theory, while the consideration of I leads to a reduction in the mid-span transverse displacements ($\overline{W}$) up to ten per cent, approximately. On the other hand, the inclusion of transverse shear effects causes a significant reduction in $\overline{\theta}$ (dimensionless angle of rotation at supports), while consideration of rotatory inertia (I) is responsible for a further decrease up to 17 per cent, approximately.

The energy partition in Figure 15 for $\nu = 1.5$ is changed significantly when the influence of transverse shear effects is included in the yield curve since fifty per cent of the initial energy is then absorbed due to shearing deformations alone when $T \geq 1/6$. The incorporation of rotatory inertia (I) in the analysis causes a further increase in the amount of energy absorbed due to transverse shear forces.

It is evident from the numerical results in Figure 16 that transverse shear effects and rotatory inertia have a negligible influence on the maximum permanent transverse displacements at the mid-span when $\nu > 4$, approximately.

6.3 General Comments

In order to avoid complete severance of the beams at the shear hinges it is necessary to ensure that the maximum shear displacements in the numerical studies are less than some proportion of the beam thickness [12].

The material was idealised as rigid perfectly plastic in this article since this characterisation gave satisfactory agreement between theoretical predictions and experimental results for many problems when the external dynamic energy was greater than about five times the strain energy which could be absorbed in a wholly elastic manner [13]. In addition, the influences of material strain rate sensitivity and geometry changes, or finite transverse displacements, were disregarded. These assumptions are probably reasonable for impulsively loaded strain rate insensitive beams when supported without axial restraints, and for infinitely long strain rate insensitive beams struck by a mass when the maximum transverse displacements are less than the beam thickness, approximately [13]. The influence of material strain hardening has been neglected in this work, but some general remarks on this topic are presented in References [13, 14].

The numerical procedure developed in this article could be used to examine the behavior of the two beam problems when governed by any convex yield criterion which relates the transverse shear force and bending moment required for plastic flow. Moreover, the numerical scheme could be employed to solve many other beam problems in an inexpensive manner and appears suffi-

ciently attractive to warrant further development in order to study the dynamic plastic response of plates and shells.

7. Conclusions

A numerical procedure has been used to examine the influence of transverse shear forces in the yield criterion and rotatory inertia on the dynamic plastic response of beams. Various results are presented for a long beam impacted by a mass and a simply supported beam loaded impulsively, both of which are made from a rigid perfectly plastic material with yielding controlled by the Ilyushin-Shapiro yield criterion.

Transverse shear effects lead to a dramatic reduction in the slopes of the deformed profiles for both beam problems. Moreover, the slope of the deformed profile underneath the striker in the impact problem is quite sensitive to the actual shape of a yield curve, while the maximum transverse displacement is less sensitive. The retention of rotatory inertia in the basic equations may lead to a further 10 per cent reduction in the slope of the impact problem, and reductions of up to 17 per cent and 10 per cent for the slopes and transverse displacements of the impulsive problem, respectively.

Acknowledgements

The authors are indebted to the Structural Mechanics Program of the Office of Naval Research who supported this work through contract number N00014-76-C 0195, Task NR 064-510.

References

1. Jones, N., and Gomes de Oliveira, J., "The Influence of Rotatory Inertia and Transverse Shear on the Dynamic Plastic Behavior of Beams," Journal of Applied Mechanics (in press).

2. Jones, N., "Recent Progress in the Dynamic Plastic Behavior of Structures," M.I.T., Department of Ocean Engineering Report Number 78-1, January 1978. The Shock and Vibration Digest, (in press).

3. Symonds, P.S., "Plastic Shear Deformations in Dynamic Load Problems," Engineering Plasticity, Edited by J. Heyman and F. A. Leckie, C.U.P., 647-664 (1968).

4. Nonaka, T., "Shear and Bending Response of a Rigid-Plastic Beam to Blast-Type Loading," Ingenieur-Archiv 46, 35-52 (1977).

5. Gomes de Oliveira, J., and Jones, N., "Some Remarks on the Influence of Transverse Shear on the Plastic Yielding of Structures," International Journal of Mechanical Science, (In Press).

6. Heyman, J., "The Full Plastic Moment of an I-Beam in the Presence of Shear Force," Journal of Mech. Physics and Solids, 18, 359-365 (1970).

7. Ilyushin, A. A., "Plasticité" (In French), Eyrolles, Paris (1956).

8. Shapiro, G. S., "On Yield Surfaces For Ideally Plastic Shells," Problems of Continuum Mechanics, SIAM, Philadelphia, 414-418 (1961).

9. Hodge, P. G., "Interaction Curves For Shear and Bending of Plastic Beams," Journal of Applied Mechanics, 24, 453-456 (1957).

10. Robinson, M., "The Effect of Transverse Shear Stresses on the Yield Surface For Thin Shells," International Journal of Solids and Structures, 9, 819-828 (1973).

11. Parkes, E.W., "The Permanent Deformation of a Cantilever Struck Transversely at its Tip," Proc. Roy. Soc. (London), 228A, 462-476 (1955).

12. Jones, N., "Plastic Failure of Ductile Beams Loaded Dynamically," Trans. ASME, J. Eng. for Ind. 98, 131-136 (1976).

13. Jones, N., "A Literature Review of the Dynamic Plastic Response of Structures," The Shock and Vibration Digest, 7 (8), 89-105 (1975).

14. Symonds, P.S., and Jones, N., "Impulsive Loading of Fully Clamped Beams with Finite Plastic Deflections and Strain Rate Sensitivity," Int. J. Mech. Sci., 14, 49-69 (1972).

List of Figures

Figure 1. Sign Convention

Figure 2. Ilyushin-Shapiro Yield Criterion and Circumscribing and Inscribing Yield Criteria for a Beam with a Rectangular Cross-Section.

Figure 3. Secant and Tangent Linearisation of Ilyushin-Shapiro Yield Criterion.

Figure 4. (a) Mass G with a Velocity V_o Striking an Infinitely Long Beam.

(b) Velocity Profile of Right Hand Half of Beam at Time t.

Figure 5. Portions of Ilyushin-Shapiro Yield Curve For Plastic Flow in Problem Shown in Figure 4(a).

Figure 6. (a) Simply Supported Beam Subjected to an Impulsive Velocity V_o.

(b) Transverse Velocity Profile.

Figure 7. Comparison of $\bar{V}$ and $\bar{V}'$ According to Ilyushin-Shapiro Yield Curve (2 and 50 facets per quadrant) with square yield curve results in Reference [3] (I=0) for an Infinitely Long Beam hit by a Mass G Travelling with an Initial Velocity V_o.

Figure 8. Infinitely Long Beam hit by a Mass G Travelling with an Initial Velocity V_o.

———————— Square Yield Curve [3]

——·——·—— Ilyushin-Shapiro Yield Curve with 50 facets per quadrant.

—— —— —— Simple Bending Solution [3]

Figure 9. Infinitely Long Beam hit by a Mass G travelling with an initial velocity V_o.

———— Ilyushin-Shapiro Yield Curve with 50 facets per quadrant and e = 0.06.

— — — Square Yield Curve [1]

① λ_o = 24.357, I = 0.4861, ② λ_o = 18.215, I = 0.4754

③ λ_o = 8.102, I = 0.4276, ④ λ_o = 3.319, I = 0.3194

Figure 10. Infinitely Long Beam hit by a Mass G travelling with an initial velocity V_o.

(a) λ_o = 3.31953.

1. Ilyushin-Shapiro Yield Curve with 50 facets per quadrant and e = 0.06, I = 0.3194

2. as 1. but with I = 0

3. Simple bending solution [3]

(b) λ_o = 24.357

1. Ilyushin-Shapiro Yield Curve with 50 facets per quadrant and e = 0.06, I = 0.4861.

2. as 1. but with I = 0

3. Simple bending solution [3]

Figure 11. Energy Ratios for an Infinitely Long Beam hit by a Mass G travelling with an initial velocity V_o. λ_o = 8.102 and I = 0.4276.

———— Ilyushin-Shapiro Yield Curve with 50 facets per quadrant and e = 0.06.

— — — Square Yield Curve [1]

Figure 12. Migration of Generalised Stresses for an Infinitely Long Beam hit by a Mass G travelling with an initial velocity V_o. λ_o = 8.102 and I = 0.4276. Ilyushin-Shapiro

yield curve with 10 facets per quadrant and e = 0.06.

—— —— —— is rigid zone shown in Figure 4(b). The time intervals refer to the plastic hinge underneath the striker.

Figure 13. Dimensionless Bending Moment ($\bar{M}$) and Transverse Shear Force ($\bar{Q}$) across the Beam in Figure 6(a) at Various Dimensionless Times (T).

$\nu = 2$, I = 0.1443, e = 0.06, $T_1 = 0.10765$ and $\alpha = x/z_1$ where $z_1 = 0.67357L$.

Figure 14. Simply Supported Beam with $\nu = 1.5$ and e = 0.06 Subjected to an Impulsive Velocity V_o.

———— $\bar{W}(T)$, —— —— —— $\bar{\theta}(T)$, x indicates $T = T_1$

① I = 0.1924, ② I = 0.1056, ③ I = 0.0521.

B: simple bending theory, S: I = 0 and e = 0 (square yield) [4].

Figure 15. Dimensionless Energy Ratios for the Simply Supported Beam in Figure 6(a) with $\nu = 1.5$ and e = 0.06 Subjected to an Impulsive Velocity V_o.

—— · —— · —— simple bending theory

—— —— —— I = 0 and e = 0 (square yield) [4],

———— I = 0.1924, x indicates $T = T_1$.

Figure 16. Variation of Maximum Permanent Transverse Displacement ($\bar{W}_T$) of Simply Supported Beam in Figure 6(a) with ν and e = 0.06.

—— · —— · —— simple bending theory

—— —— —— I = 0 and e = 0 (square yield) [4].

① $I\nu = 0.2886$, ② $I\nu = 0.1584$,

③ $I\nu = 0.0781$, ④ $I\nu = 0.0600$

Figure 17. Migration of Generalised Stresses in the Simply Supported Beam in Figure 6(a).

$\nu = 2$, $I = 0.1443$, $e = 0.06$, $T_1 = 0.10765$.

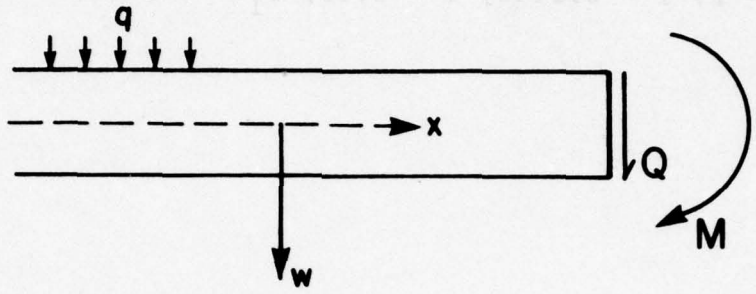

FIGURE 1

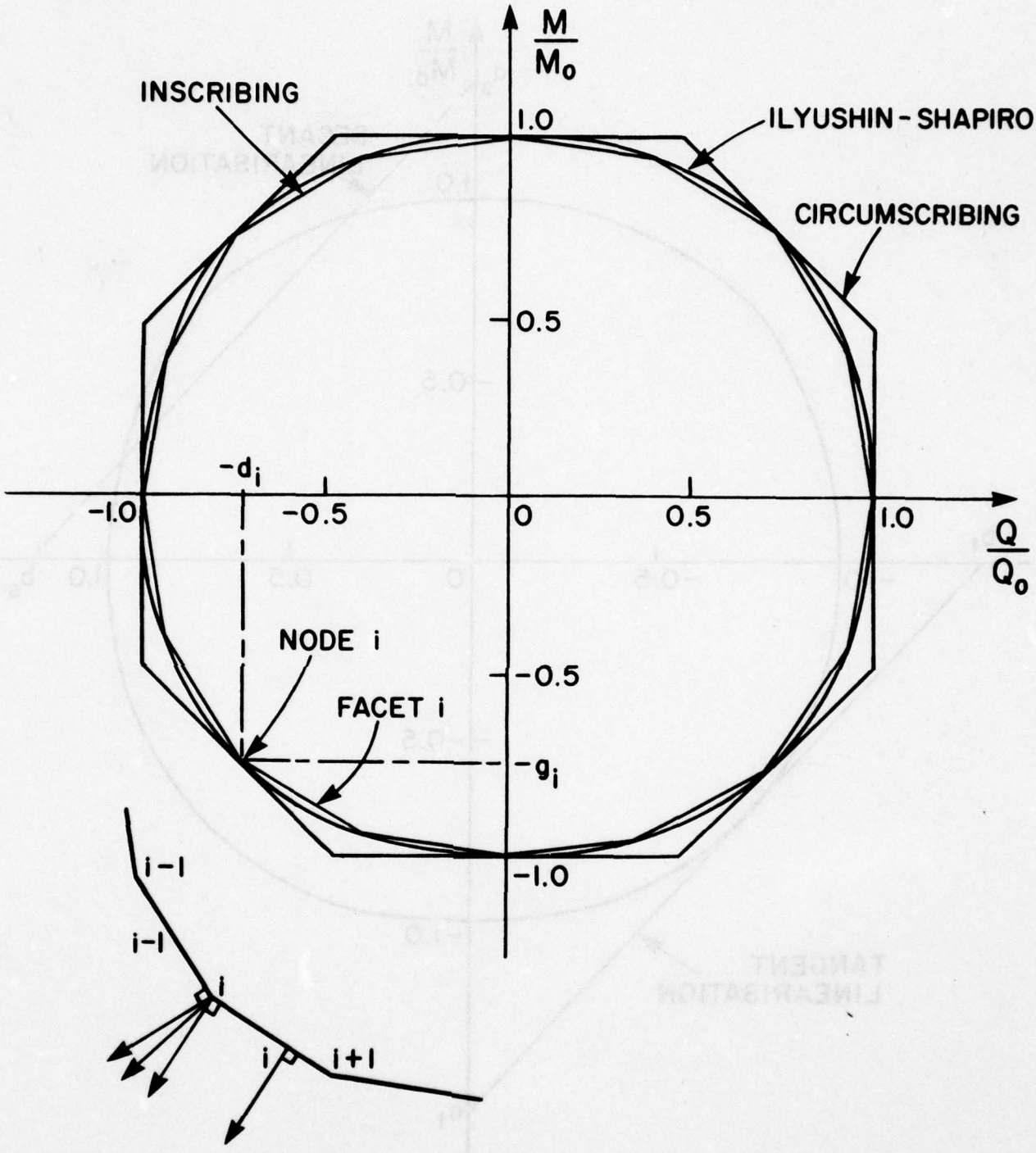
M/M0
INSCRIBING
1.0
ILYUSHIN - SHAPIRO
CIRCUMSCRIBING
0.5
-di
-1.0
-0.5
0
0.5
1.0
Q/Q0
NODE i
-0.5
FACET i
-gi
-1.0
i-1
i-1
i
i
i+1

FIGURE 2

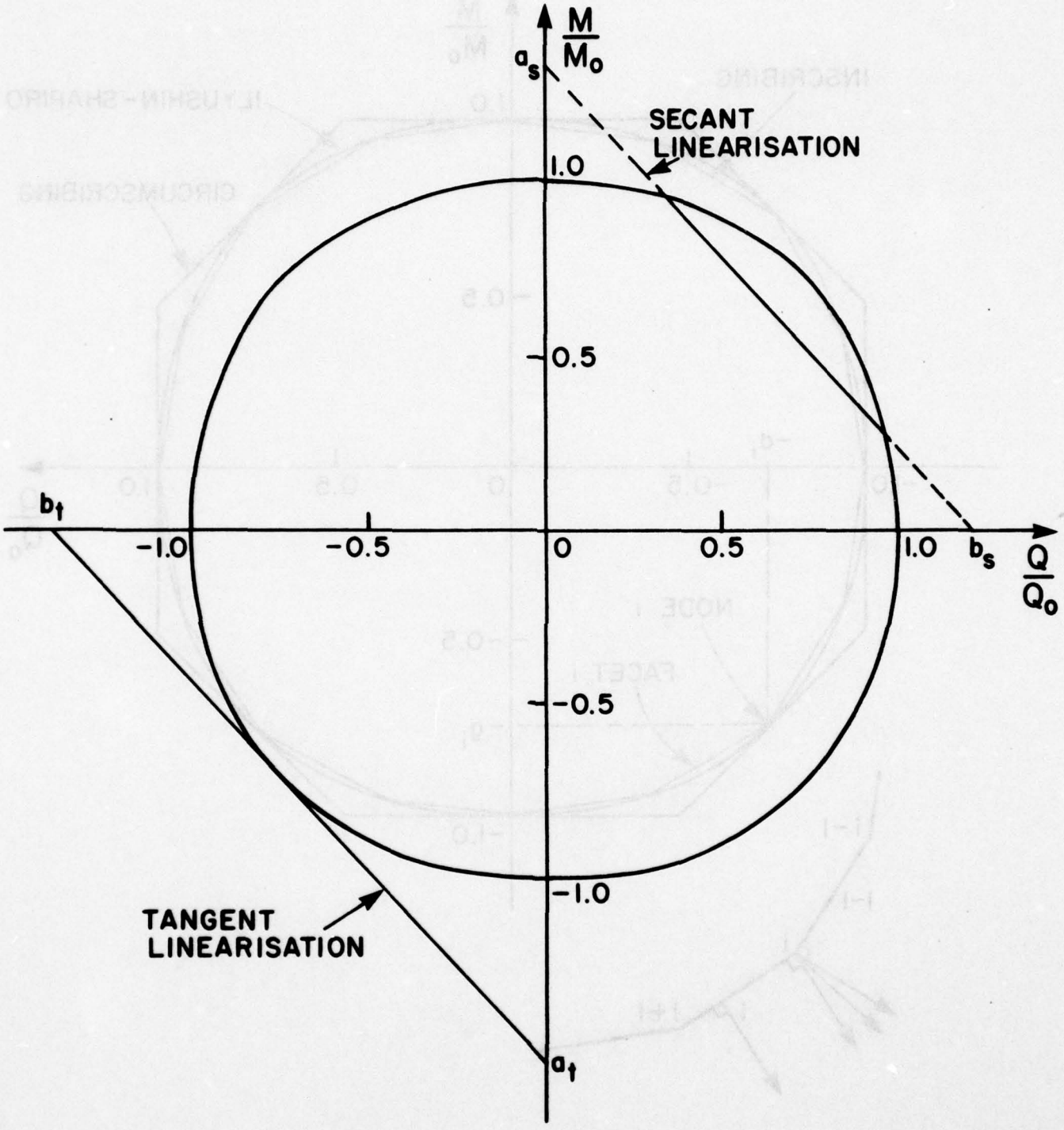
M/M0
as
SECANT
LINEARISATION
1.0
0.5
bf
-1.0
-0.5
0
0.5
1.0
bs
Q/Q0
-0.5
-1.0
TANGENT
LINEARISATION
af

FIGURE 3

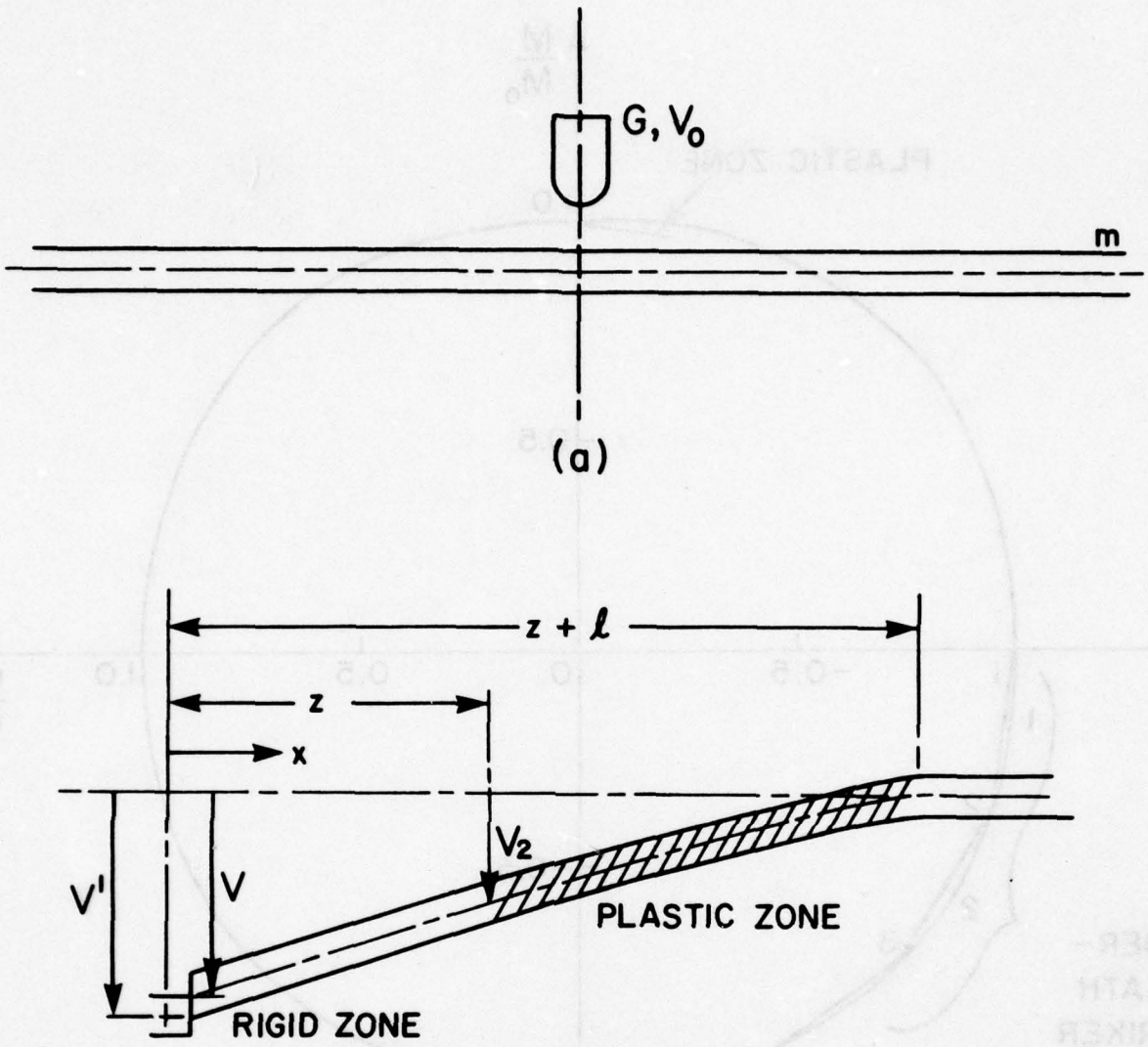

FIGURE 4

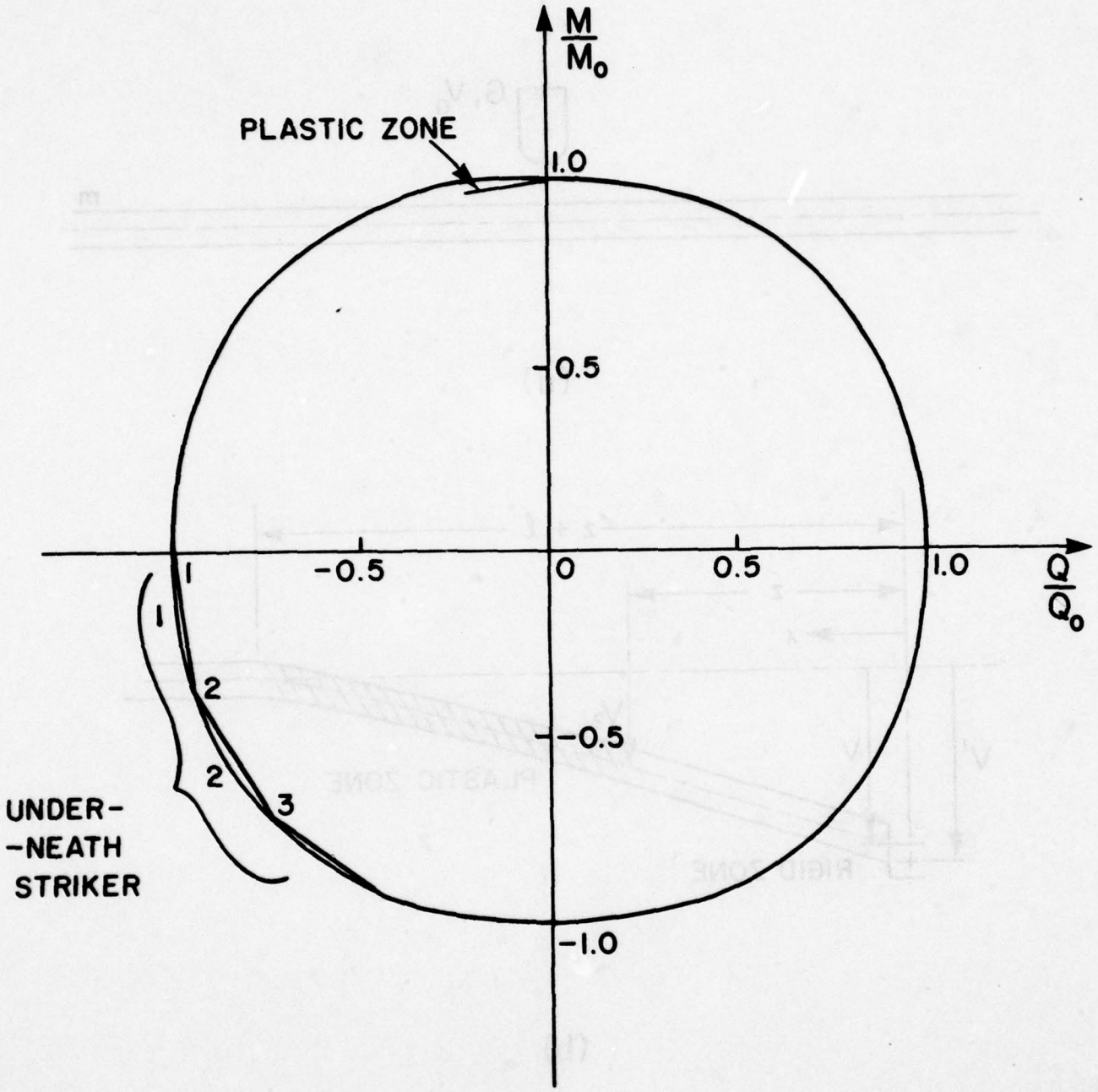
M/M0
PLASTIC ZONE
1.0
0.5
-0.5
0
0.5
1.0
Q/Q0
-0.5
-1.0
1
2
2
3
UNDER-
-NEATH
STRIKER

FIGURE 5

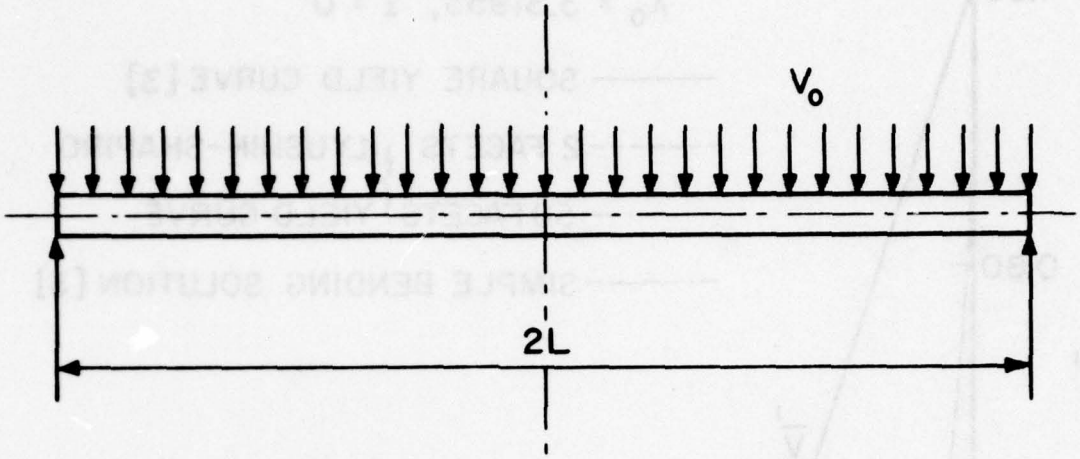

(a)

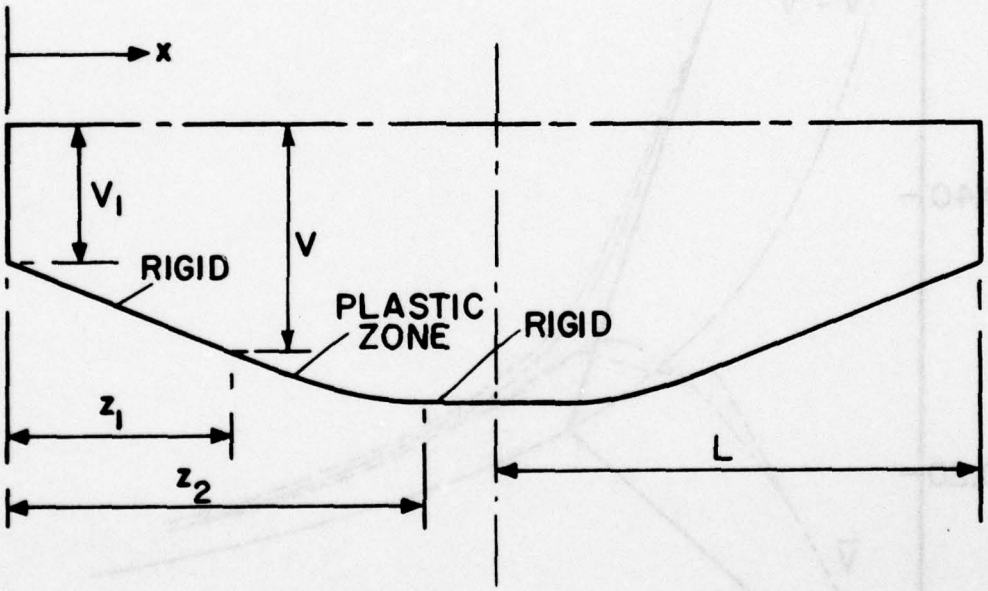

(b)

FIGURE 6

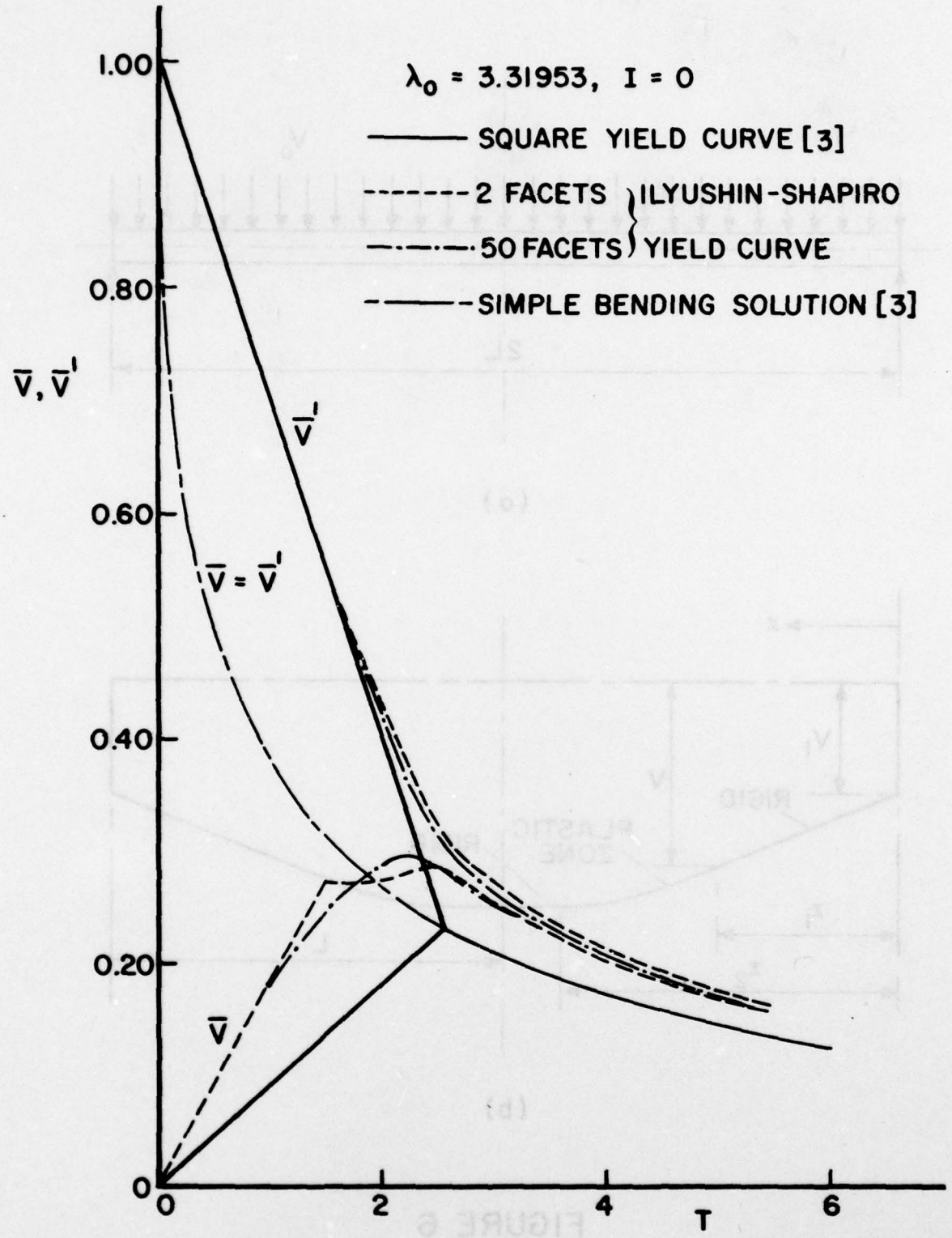
λ_0 = 3.31953, I = 0
SQUARE YIELD CURVE [3]
2 FACETS
50 FACETS
ILYUSHIN-SHAPIRO YIELD CURVE
SIMPLE BENDING SOLUTION [3]
$\bar{V}, \bar{V}'$
1.00
0.80
0.60
0.40
0.20
0
$\bar{V}'$
$\bar{V} = \bar{V}'$
$\bar{V}$
0
2
4
6
T

FIGURE 7

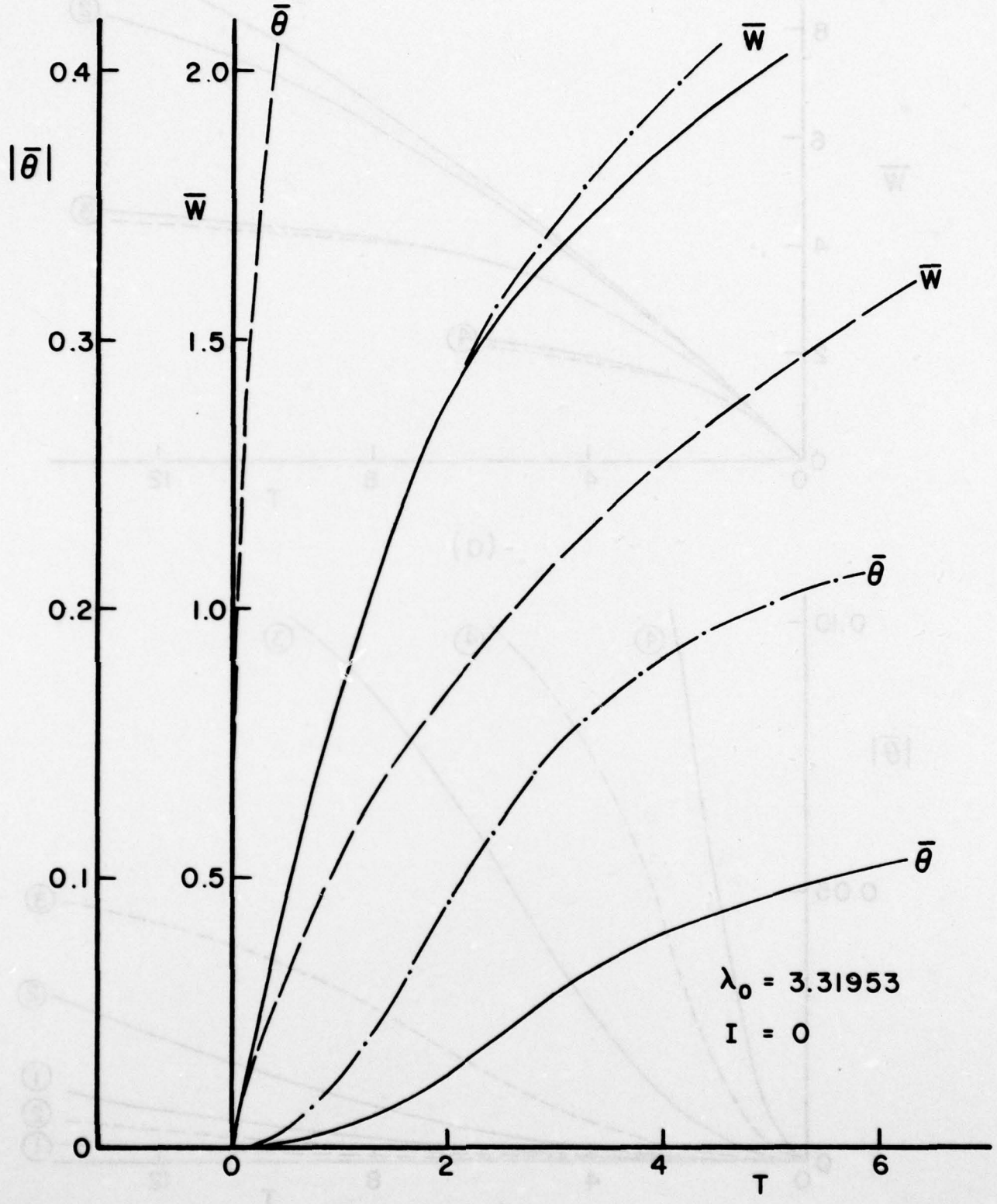
$\bar{\theta}$
$\bar{W}$
$\bar{W}$
$\bar{\theta}$
$\bar{\theta}$
$|\bar{\theta}|$
$\bar{W}$
0.4
0.3
0.2
0.1
0
2.0
1.5
1.0
0.5
0
2
4
6
T
$\lambda_0 = 3.31953$
I = 0

FIGURE 8

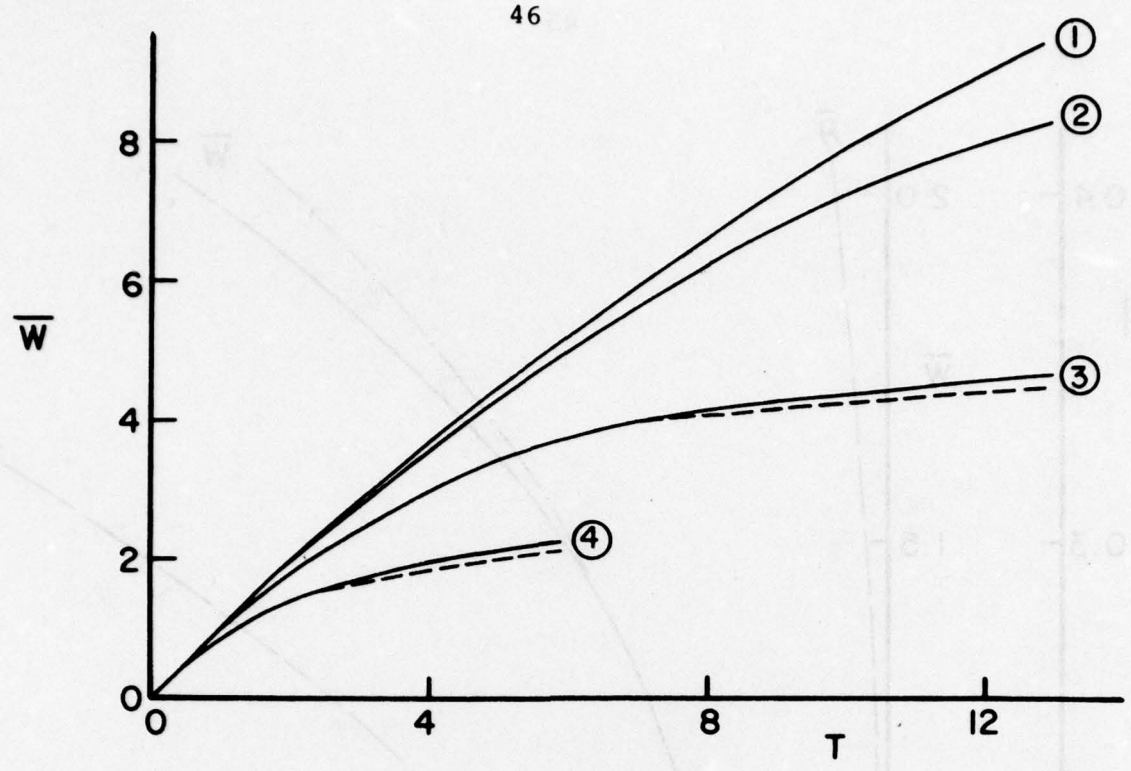
$\overline{W}$
8
6
4
2
0
0
4
8
12
T
①
②
③
④

(a)

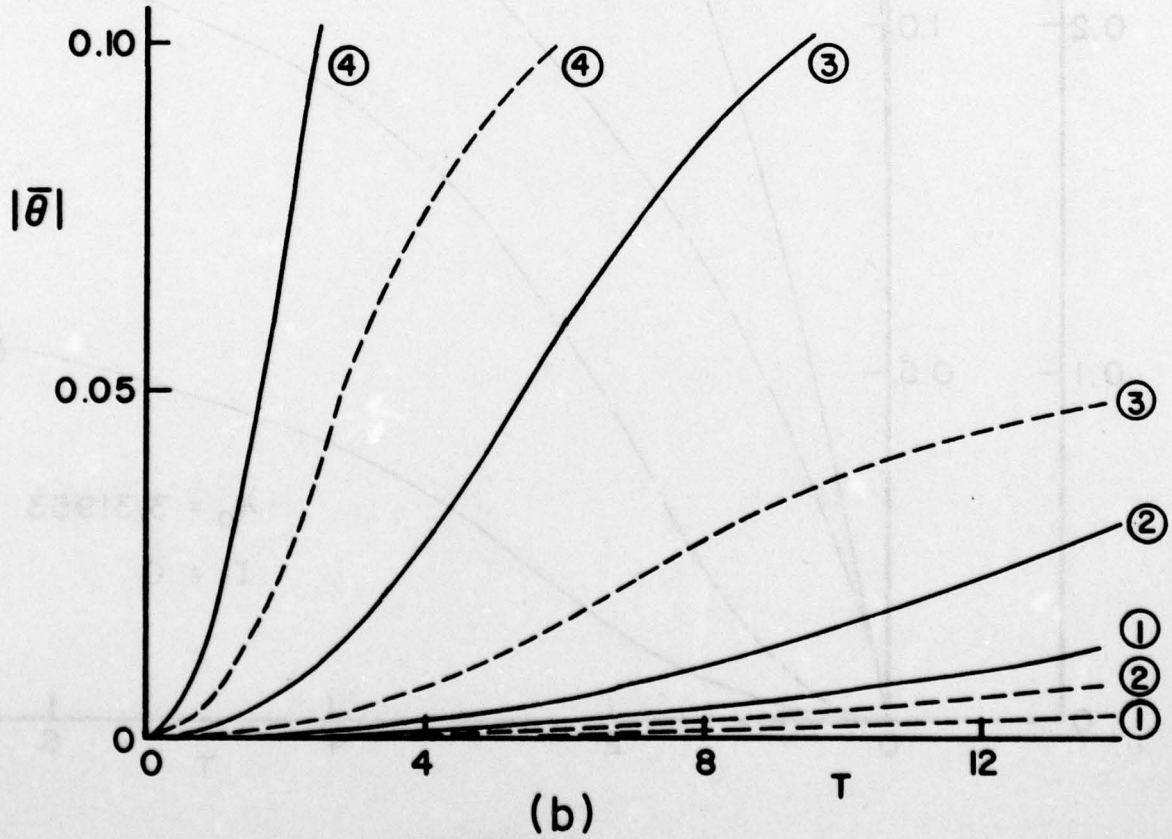
$|\bar{\theta}|$
0.10
0.05
0
0
4
8
12
T
④
④
③
③
②
①
②
①

(b)

FIGURE 9

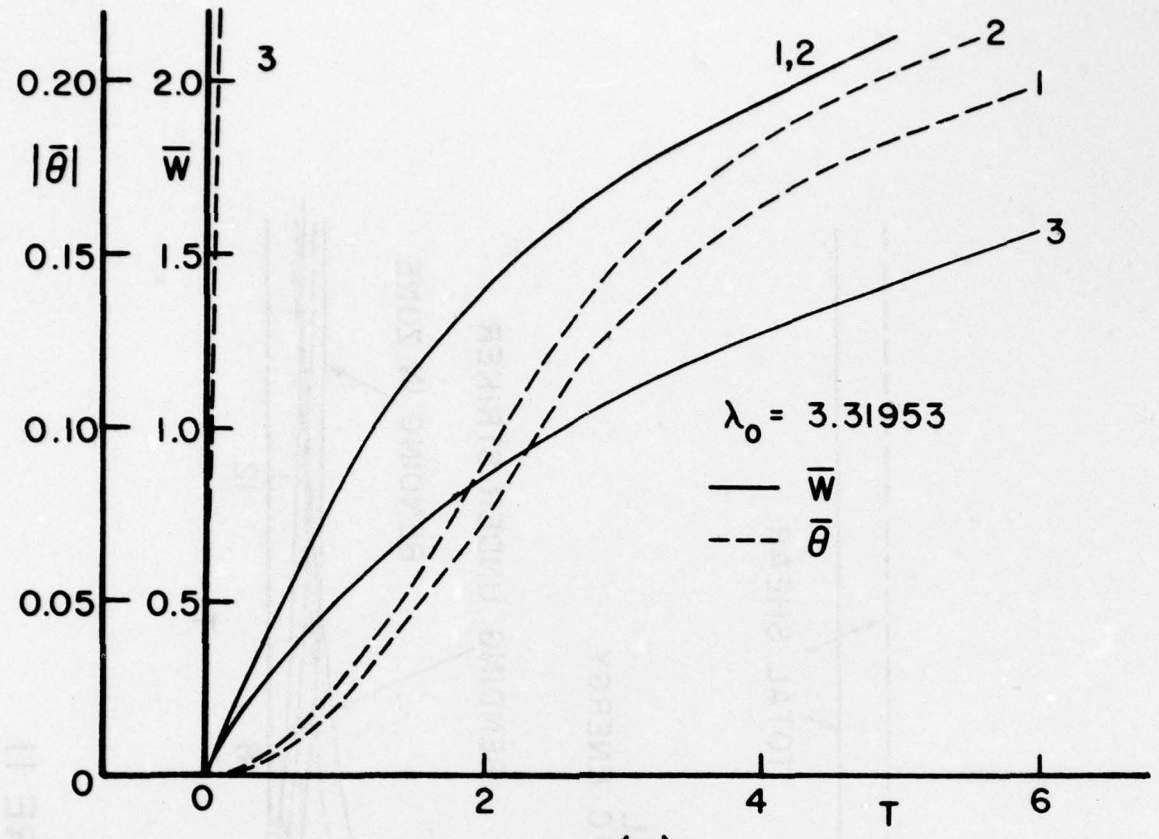
0.20
2.0
3
1,2
2
1
|θ̄|
w̄
0.15
1.5
3
0.10
1.0
λ0 = 3.31953
w̄
θ̄
0.05
0.5
0
0
2
4
T
6

(a)

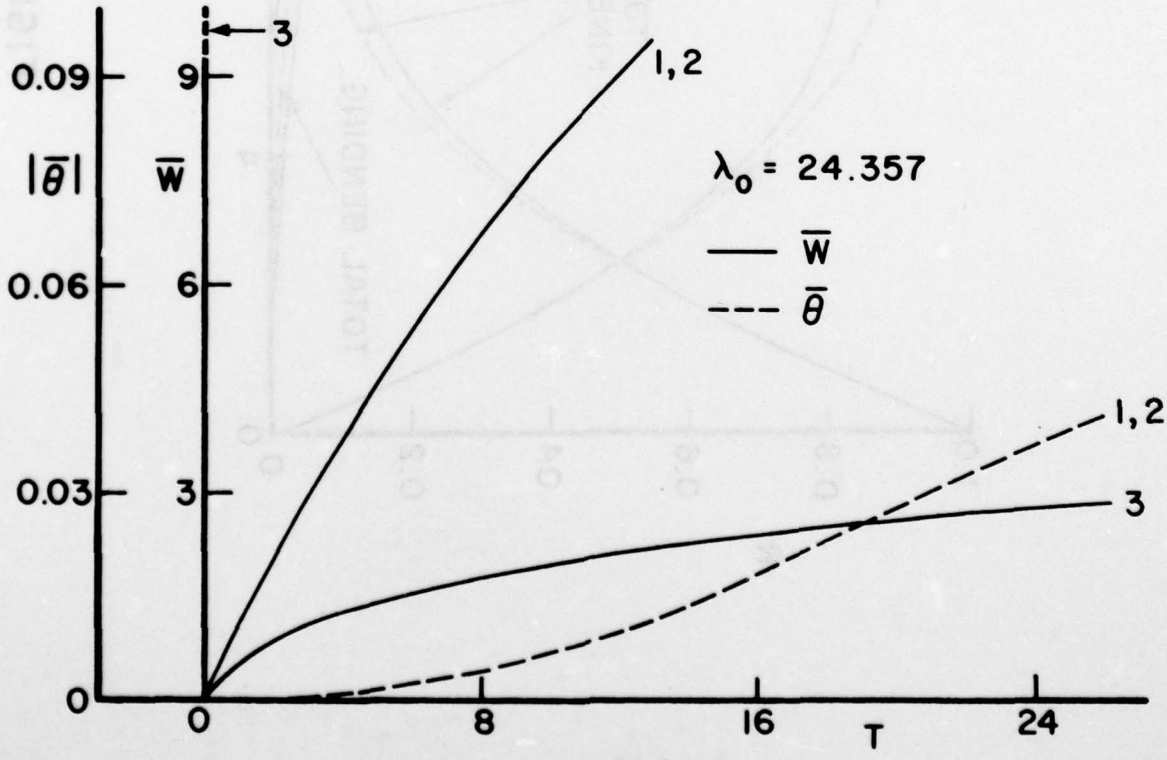
3
0.09
9
1,2
|θ̄|
w̄
λ0 = 24.357
w̄
θ̄
0.06
6
1,2
0.03
3
3
0
0
8
16
T
24

(b)

FIGURE 10

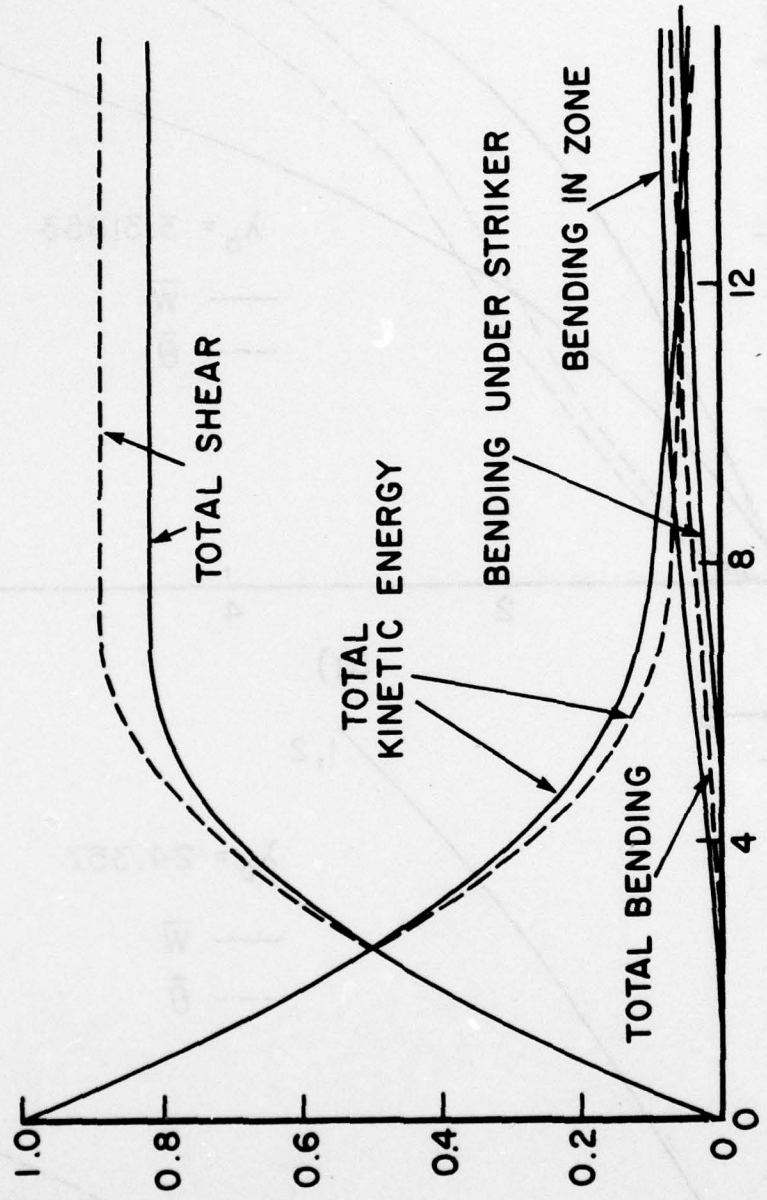
1.0
0.8
0.6
0.4
0.2
0
R
0
4
8
12
T
TOTAL SHEAR
TOTAL KINETIC ENERGY
BENDING UNDER STRIKER
BENDING IN ZONE
TOTAL BENDING

FIGURE 11

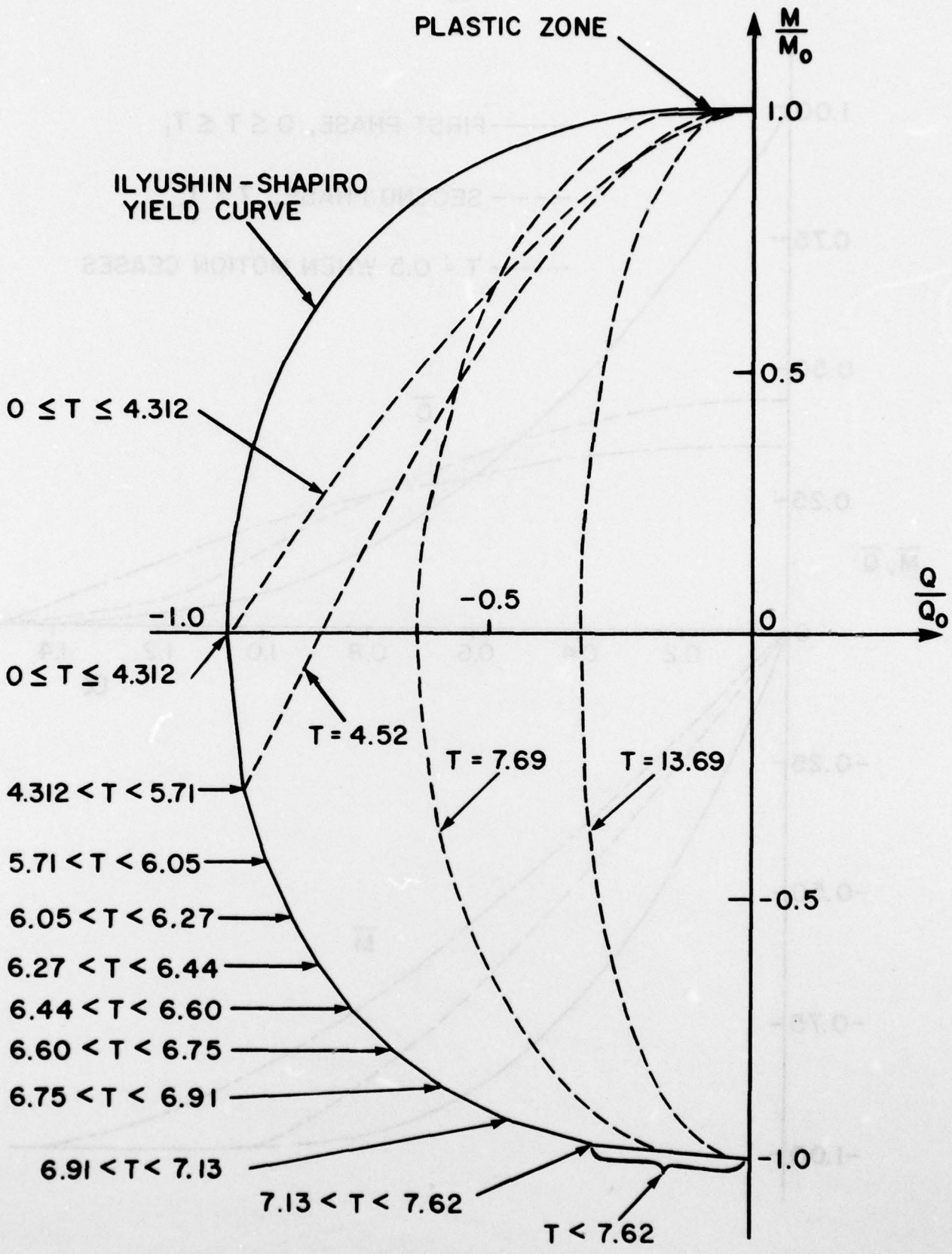
PLASTIC ZONE
M/M0
1.0
ILYUSHIN-SHAPIRO
YIELD CURVE
0.5
0 ≤ T ≤ 4.312
-1.0
-0.5
0
Q/Q0
0 ≤ T ≤ 4.312
T = 4.52
T = 7.69
T = 13.69
4.312 < T < 5.71
5.71 < T < 6.05
6.05 < T < 6.27
6.27 < T < 6.44
6.44 < T < 6.60
6.60 < T < 6.75
6.75 < T < 6.91
-0.5
6.91 < T < 7.13
-1.0
7.13 < T < 7.62
T < 7.62

FIGURE 12

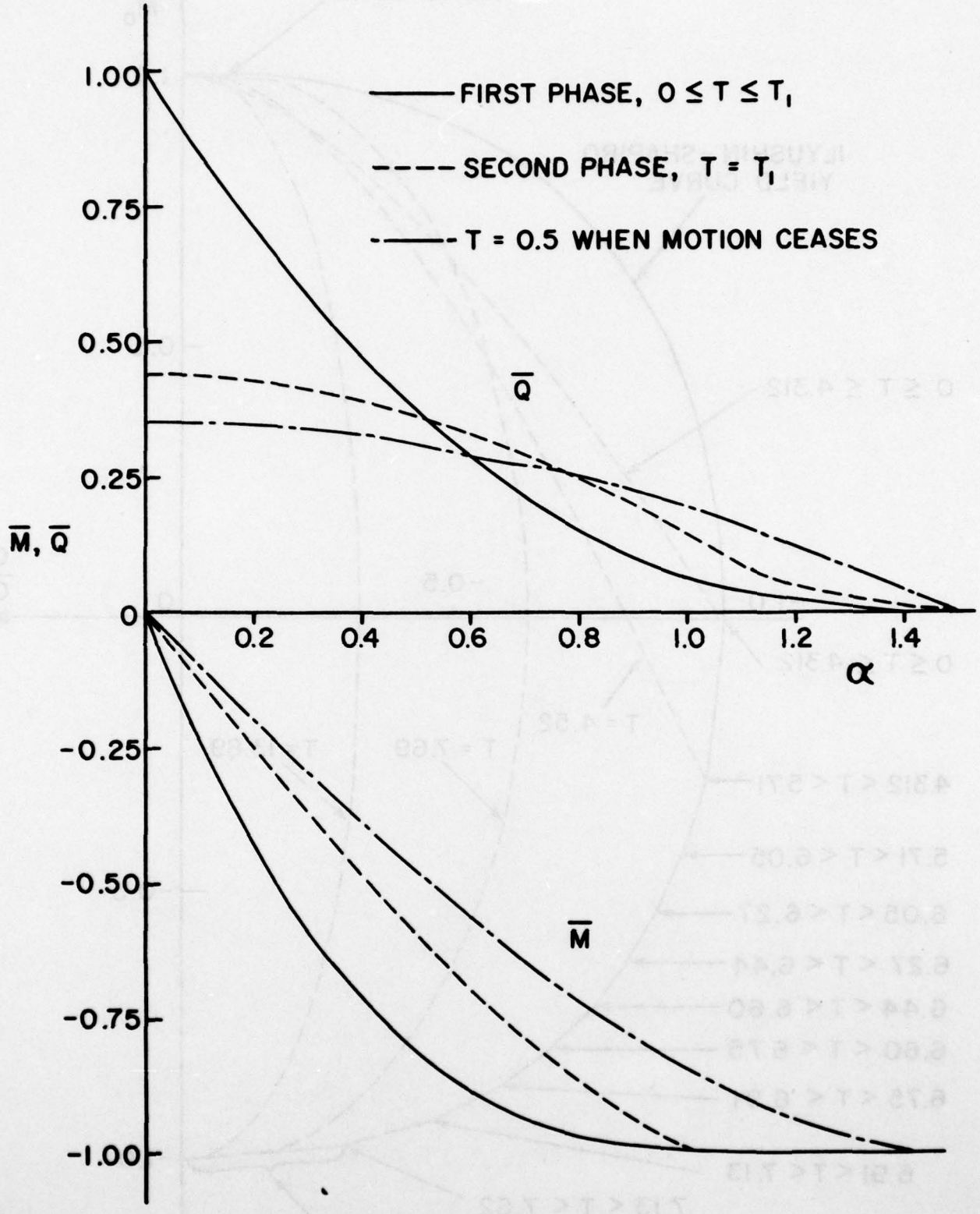
FIRST PHASE, $0 \leq T \leq T_1$
SECOND PHASE, $T = T_1$
T = 0.5 WHEN MOTION CEASES
$\overline{Q}$
$\overline{M}$
$\overline{M}, \overline{Q}$
α
1.00
0.75
0.50
0.25
0
-0.25
-0.50
-0.75
-1.00
0.2
0.4
0.6
0.8
1.0
1.2
1.4

FIGURE 13

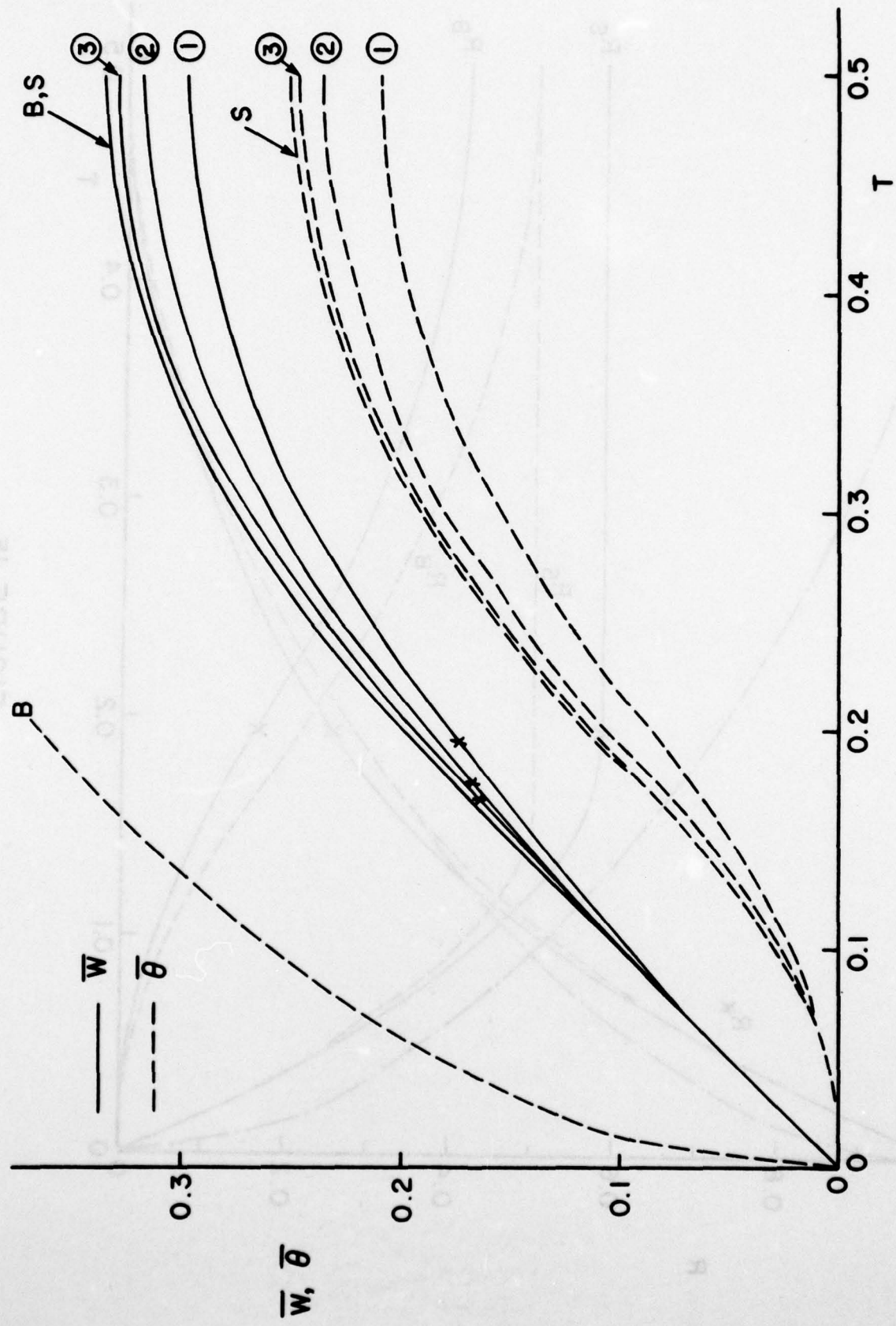
B,S
③
②
①
S
③
②
①
B
$\overline{W}$
$\overline{\theta}$
$\overline{W}, \overline{\theta}$
0.3
0.2
0.1
0
0
0.1
0.2
0.3
0.4
0.5
T

FIGURE 14

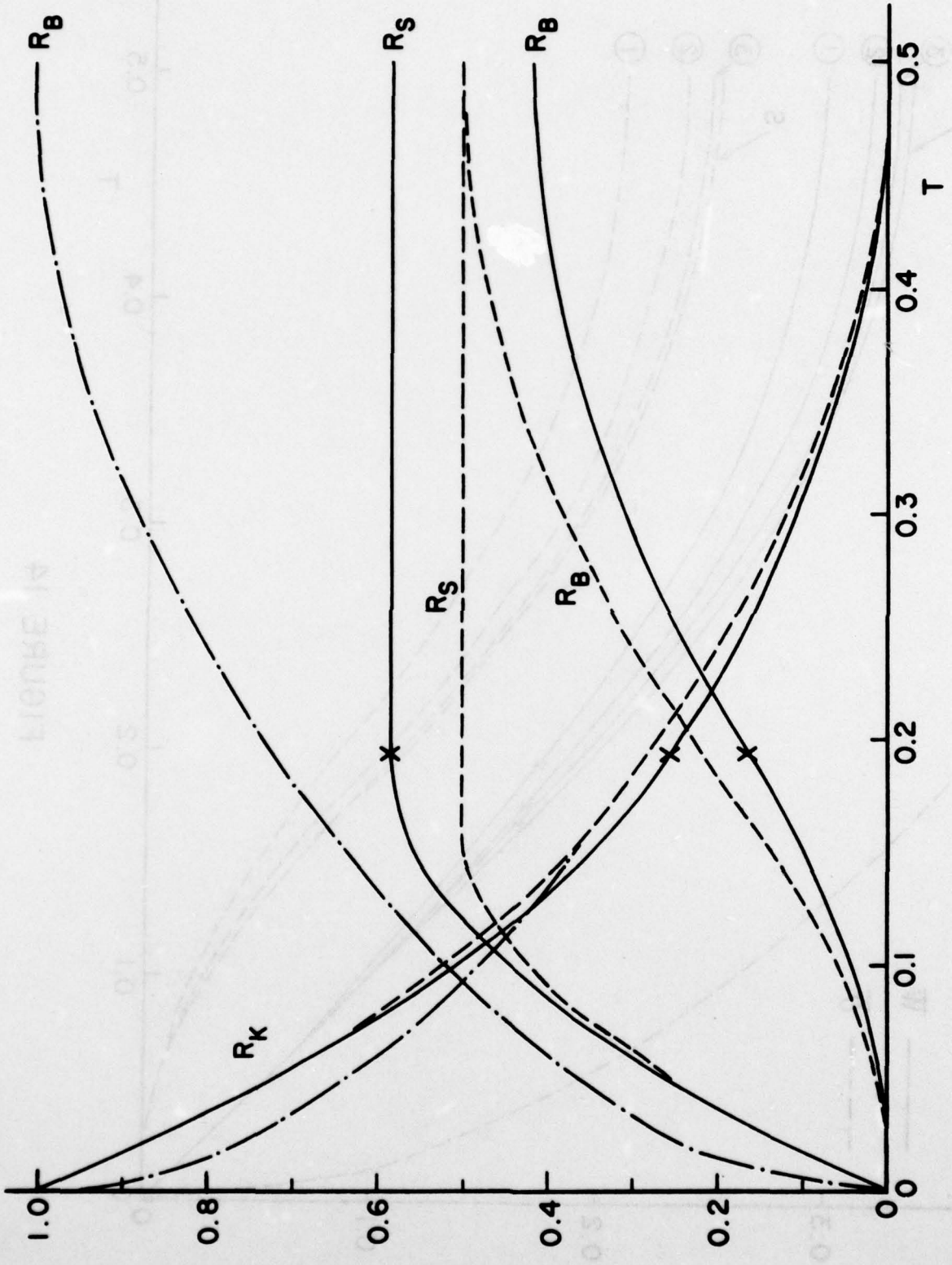

FIGURE 15

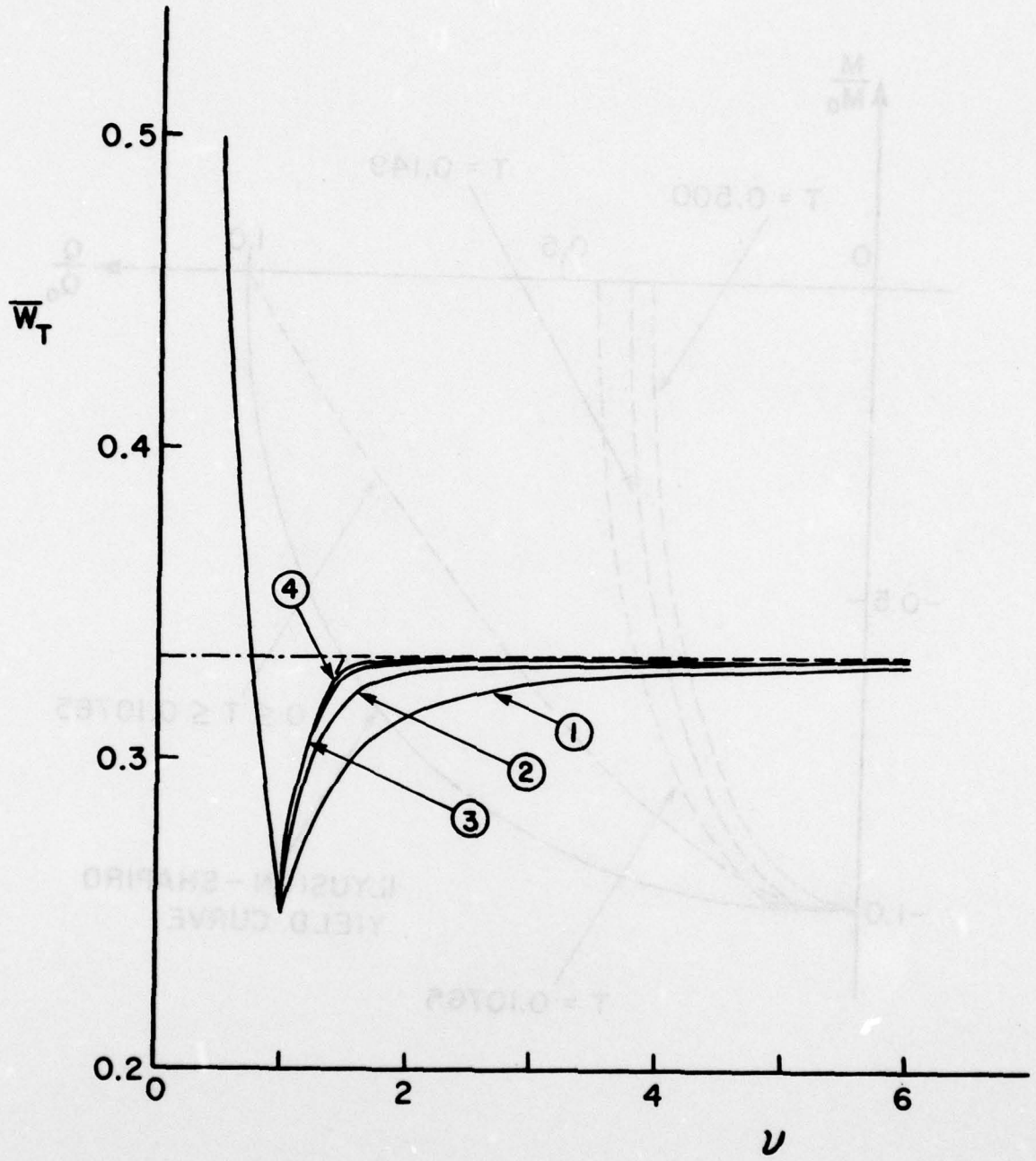

FIGURE 16

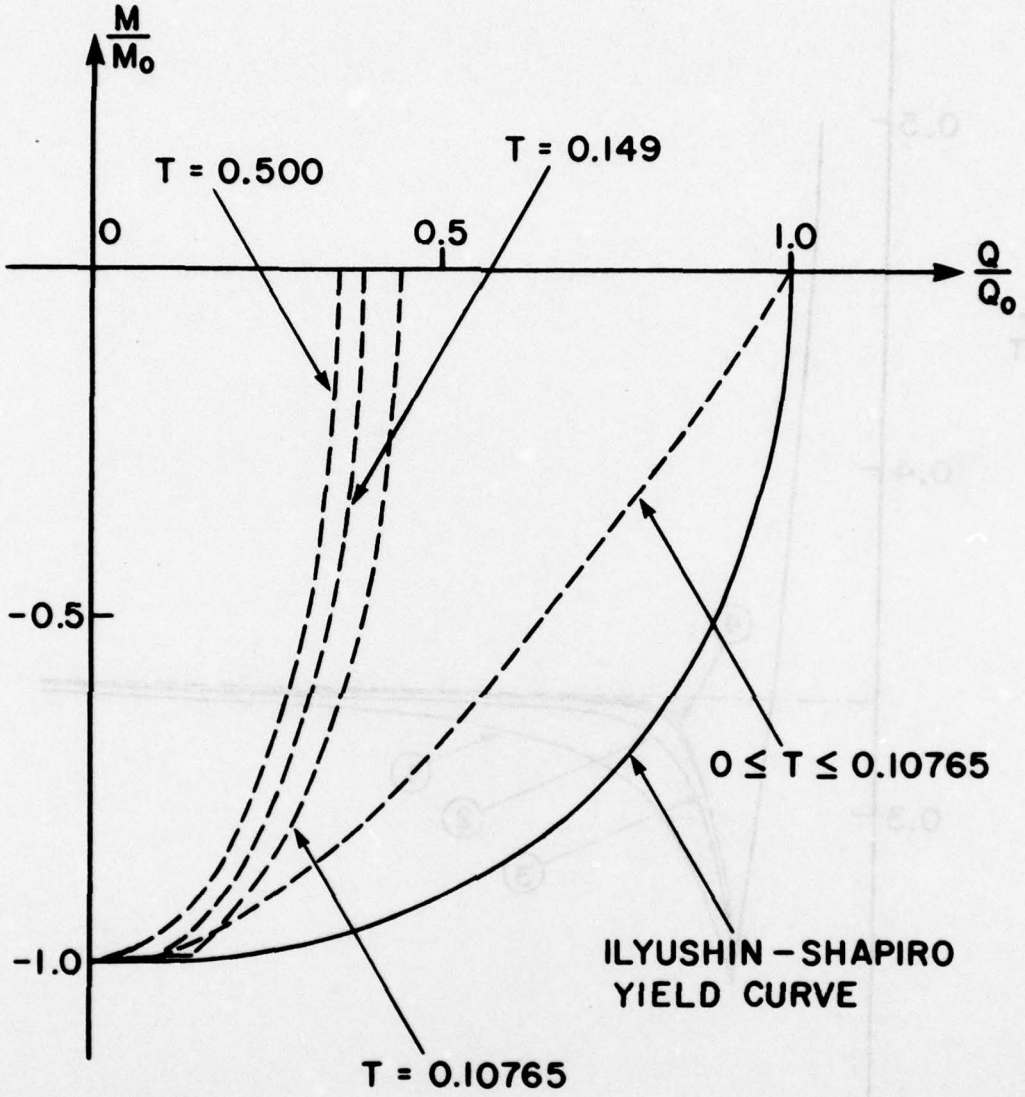
M/M0
T = 0.500
T = 0.149
0
0.5
1.0
Q/Q0
-0.5
-1.0
0 ≤ T ≤ 0.10765
ILYUSHIN – SHAPIRO
YIELD CURVE
T = 0.10765

FIGURE 17

UNCLASSIFIED

SECURITY CLASSIFICATION OF THIS PAGE (When Data Entered)

REPORT DOCUMENTATION PAGE		READ INSTRUCTIONS BEFORE COMPLETING FORM
1. REPORT NUMBER 78-2	2. GOVT ACCESSION NO.	3. RECIPIENT'S CATALOG NUMBER 54
4. TITLE (and Subtitle) A Numerical Procedure for the Dynamic Plastic Response of Beams with Rotatory Inertia and Transverse Shear Effects		5. TYPE OF REPORT & PERIOD COVERED Interim 6. PERFORMING ORG. REPORT NUMBER 78-2
7. AUTHOR(s) J. Gomes de Oliveira and Norman Jones		8. CONTRACT OR GRANT NUMBER(s) N00014-76-C-0195 Task NR 064-510
9. PERFORMING ORGANIZATION NAME AND ADDRESS Massachusetts Institute of Technology Cambridge, Massachusetts 02139 Department of Ocean Engineering		10. PROGRAM ELEMENT, PROJECT, TASK AREA & WORK UNIT NUMBERS
11. CONTROLLING OFFICE NAME AND ADDRESS Structural Mechanics Program O.N.R. Arlington, VA 22217		12. REPORT DATE August 1978 13. NUMBER OF PAGES
14. MONITORING AGENCY NAME & ADDRESS(if different from Controlling Office)		15. SECURITY CLASS. (of this report) UNCLASSIFIED 15a. DECLASSIFICATION/DOWNGRADING SCHEDULE

16. DISTRIBUTION STATEMENT (of this Report)

This document has been approved for public release and sale: Distribution unlimited.

17. DISTRIBUTION STATEMENT (of the abstract entered in Block 20, if different from Report)

18. SUPPLEMENTARY NOTES

19. KEY WORDS (Continue on reverse side if necessary and identify by block number)

rotatary inertia
shear
dynamic
plastic
beams

20. ABSTRACT (Continue on reverse side if necessary and identify by block number)

A numerical procedure is used to examine the influence of transverse shear forces in the yield criterion and rotatory inertia on the dynamic plastic response of beams. Various results are presented for a long beam impacted by a mass and a simply supported beam loaded impulsively, both of which are made from a rigid perfectly plastic material with yielding controlled by the Ilyushin-Shapiro yield criterion.

DD FORM 1 JAN 73 1473 EDITION OF 1 NOV 65 IS OBSOLETE

S/N 0102-LF-014-6601

UNCLASSIFIED

SECURITY CLASSIFICATION OF THIS PAGE (When Data Entered)

Transverse shear effects lead to a dramatic reduction in the slopes of the deformed profiles for both beam problems. Moreover, the slope of the deformed profile underneath the striker in the impact problem is quite sensitive to the actual shape of the yield curve, while the maximum transverse displacement is less sensitive. The retention of rotatory inertia in the basic equations leads to further reductions up to 17 and 10 per cent in the slopes and maximum transverse displacements, respectively.

M.I.T. Department of Ocean Engineering

Report No. 78-2

A Numerical Procedure for the Dynamic Plastic Response of Beams with Rotatory Inertia and Transverse Shear Effects, By J. Gomes de Oliveira and Norman Jones, February 1978.

A numerical procedure is used to examine the influence of transverse shear forces in the yield criterion and rotatory inertia on the dynamic plastic response of beams. Various results are presented for a long beam impacted by a mass and a simply supported beam loaded impulsively, both of which are made from a rigid perfectly plastic material with yielding controlled by the Ilyushin-Shapiro yield criterion.

Transverse shear effects lead to a dramatic reduction in the slopes of the deformed profiles for both beam problems. Moreover, the slope of the deformed profile underneath the striker in the impact problem is quite sensitive to the actual shape of a yield curve, while the maximum transverse displacement is less sensitive. The retention of rotatory inertia in the basic equations leads to further reductions up to 17 and 10 per cent in the slopes and maximum transverse displacements, respectively.

rotatory inertia
shear
dynamic
plastic
beams

M.I.T. Department of Ocean Engineering

Report No. 78-2

A Numerical Procedure for the Dynamic Plastic Response of Beams with Rotatory Inertia and Transverse Shear Effects, By J. Gomes de Oliveira and Norman Jones, February 1978.

A numerical procedure is used to examine the influence of transverse shear forces in the yield criterion and rotatory inertia on the dynamic plastic response of beams. Various results are presented for a long beam impacted by a mass and a simply supported beam loaded impulsively, both of which are made from a rigid perfectly plastic material with yielding controlled by the Ilyushin-Shapiro yield criterion.

Transverse shear effects lead to a dramatic reduction in the slopes of the deformed profiles for both beam problems. Moreover, the slope of the deformed profile underneath the striker in the impact problem is quite sensitive to the actual shape of a yield curve, while the maximum transverse displacement is less sensitive. The retention of rotatory inertia in the basic equations leads to further reductions up to 17 and 10 per cent in the slopes and maximum transverse displacements, respectively.

rotatory inertia
shear
dynamic
plastic
beams

M.I.T. Department of Ocean Engineering

Report No. 78-2

A Numerical Procedure for the Dynamic Plastic Response of Beams with Rotatory Inertia and Transverse Shear Effects, By J. Gomes de Oliveira and Norman Jones, February 1978.

A numerical procedure is used to examine the influence of transverse shear forces in the yield criterion and rotatory inertia on the dynamic plastic response of beams. Various results are presented for a long beam impacted by a mass and a simply supported beam loaded impulsively, both of which are made from a rigid perfectly plastic material with yielding controlled by the Ilyushin-Shapiro yield criterion.

Transverse shear effects lead to a dramatic reduction in the slopes of the deformed profiles for both beam problems. Moreover, the slope of the deformed profile underneath the striker in the impact problem is quite sensitive to the actual shape of a yield curve, while the maximum transverse displacement is less sensitive. The retention of rotatory inertia in the basic equations leads to further reductions up to 17 and 10 per cent in the slopes and maximum transverse displacements, respectively.

rotatory inertia
shear
dynamic
plastic
beams

M.I.T. Department of Ocean Engineering

Report No. 78-2

A Numerical Procedure for the Dynamic Plastic Response of Beams with Rotatory Inertia and Transverse Shear Effects, By J. Gomes de Oliveira and Norman Jones, February 1978.

A numerical procedure is used to examine the influence of transverse shear forces in the yield criterion and rotatory inertia on the dynamic plastic response of beams. Various results are presented for a long beam impacted by a mass and a simply supported beam loaded impulsively, both of which are made from a rigid perfectly plastic material with yielding controlled by the Ilyushin-Shapiro yield criterion.

Transverse shear effects lead to a dramatic reduction in the slopes of the deformed profiles for both beam problems. Moreover, the slope of the deformed profile underneath the striker in the impact problem is quite sensitive to the actual shape of a yield curve, while the maximum transverse displacement is less sensitive. The retention of rotatory inertia in the basic equations leads to further reductions up to 17 and 10 per cent in the slopes and maximum transverse displacements, respectively.

rotatory inertia
shear
dynamic
plastic
beams